Tetrahydrobiopterin Radical Enzymology

ARTICLE *in* CHEMICAL REVIEWS · JULY 2003

Impact Factor: 46.57 · DOI: 10.1021/cr0204350 · Source: PubMed

3 AUTHORS, INCLUDING:

Chin-Chuan Wei
Southern Illinois University Edwardsville
43 PUBLICATIONS **1,399** CITATIONS
SEE PROFILE

Dennis J Stuehr
Cleveland Clinic
315 PUBLICATIONS **26,706** CITATIONS
SEE PROFILE

Tetrahydrobiopterin Radical Enzymology

Chin-Chuan Wei,[†] Brian R. Crane,[‡] and Dennis J. Stuehr*,[†]

Department of Immunology, The Lerner Research Institute, Cleveland Clinic Foundation, Cleveland, Ohio 44195, and Department of Chemistry and Chemical Biology, Cornell University, Ithaca, New York 14853

Received October 31, 2002

Contents

I. Introduction

(6*R*)-5,6,7,8-Tetrahydrobiopterin (H_4B) and related tetrahydropterins are cofactors for several enzymes and can be generators or scavengers of reactive oxygen species in cells. Our review will focus on pterin radical formation in enzymes, particularly in the nitric oxide synthases (NOSs, EC 1.14.13.39) where pterin radical formation is best documented. We also summarize properties of pterin and pterin radicals that are generated in chemical systems and compare and contrast structure−function aspects of several H_4B-utilizing enzymes in an effort to provide perspective for understanding H_4B radical formation in enzymes.

Reviews on biosynthesis, regulation, and functions of H_4B and related tetrahydropterins are available.[1,2] Redox function of H_4B in the aromatic amino acid hydroxylase enzymes (AAH) has also been covered in recent reviews,[3−5] and recent reviews on H_4B redox function in NOSs are available.[6,7] Various aspects of pterin chemistry have also been reviewed.[8]

II. Chemistry of Pterin

A. Chemical Properties of Pterin

Biopterin is a member of a family that includes pterins, lumazines, alloxazines, folates, and riboflavins. All of these molecules have a core structure of two or three heterocyclic six-membered rings (Figure 1).

Spectroscopic properties of pterins in their various oxidation and protonation states are well documented.[9,10] In solution pterins populate different tautomers according to the pH. Figure 2 shows protonation of the pterin nitrogen (amide group) and phenolate groups as a function of pH. The pK_a of N1 and N5 are 1.3 and 5.6,[9] so that at physiologic pH, biopterin primarly exists as an uncharged species. Biopterin in its various oxidation states is shown in Figure 3. Heteroatom protonation follows the same order in both the dihydo and tetrahydro forms of pterin.[9] The protonation state is thought to be an important parameter that regulates biopterin binding and function in enzymes.

Pterins can form redox-active metal chelates through the O4 and N5 atoms, and information on pterin−metal interactions and spectral and electrochemical properties of the various coordination complexes is available in a recent review.[11] Structures of metal complexes with pteridine and alloxazine mostly involved coordination of O(4)−C(4)−C(4a)−N(5)−M to form a five-membered ring.[11] However, it is now appreciated that such complexes do not mimic how pterin coenzymes coordinate with molybdenum and tungsten atoms that are bound in a number of enzymes. For example, molybdopterin or tungstopterin coenzyme contains Mo or W bound by a dithiolene moiety attached to the pterin.

Tetrahydropterins such as H_4B are labile in solution and can react with O_2,[12] superoxide,[13] H_2O_2,[9] and peroxynitrite.[14] Accordingly, H_4B has been suggested

* To whom correspondence should be addressed. Phone: 216-445-6950. Fax: 216-444-9329. E-mail: stuehrd@ccf.org.
[†] The Lerner Research Institute, Cleveland Clinic Foundation.
[‡] Cornell University.

10.1021/cr0204350 CCC: $44.00
Published on Web 05/06/2003

Chin-Chuan Wei received his B.Sc. degree in Chemistry from National Sun Yat-Sen University in Taiwan (1988) and his Ph.D. degree in Biophysical Chemistry from City University of New York (1998). In his Ph.D. studies he worked on the mechanistic studies of protein biosynthesis with Dixie J. Goss. He then join the research teams at Cleveland Clinic Foundation, working on the structural and functional studies of natriuretic peptide receptor and nitric oxide synthase. He is currently a Fellow of the American Heart Association and a Project Staff in the Immunology Department of the Cleveland Clinic Foundation.

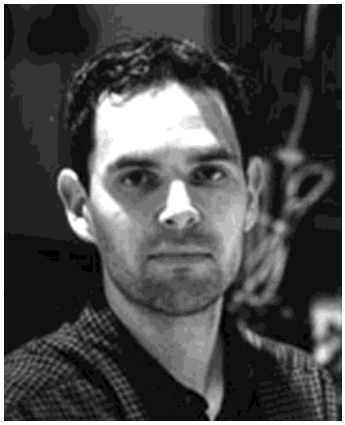

Brian R. Crane was born in Winnipeg Manitoba (1968). He received his B.Sc. degree (1990) from the University of Manitoba in Biochemistry and his Ph.D. degree (1996) from The Scripps Research Institute in Macromolecular and Cellular Structure and Chemistry. As a graduate student he worked on structural and biochemical studies of sulfite reductase and nitric oxide synthase with Elizabeth D. Getzoff and John A. Tainer. He then moved to the California Institute of Technology as a Helen Hay Whitney Postdoctoral Fellow under Harry B. Gray. At Caltech, Dr. Crane studied electron-transfer reactions in metalloproteins with Gray and J. R. Winkler and developed methods for photoinitiating redox chemistry in protein crystals. He is currently Assistant Professor and Searle Scholar in the Department of Chemistry and Chemical Biology at Cornell University. Research interests include metalloenzyme structure and function, protein electron transfer, and redox reactions involved in biological signal transduction.

Dennis J. Stuehr was born in Cleveland, OH, in 1958 and received his B.S. degree in Chemistry from Bowling Green State University in 1980. He completed his Ph.D. degree in Toxicology with Dr. Michael Marletta at The Massachusetts Institute of Technology in 1987, during which time they, in collaboration with Dr. Steven Tannenbaum, performed some of the earliest investigations into mammalian nitrogen oxide biosynthesis. In 1987 he moved to Cornell University Medical College and continued his work as a Leukemia Society Fellow with Dr. Carl Nathan in the Department of Medicine. He joined the faculty in 1989 as Assistant Professor and then moved, in 1991, to The Cleveland Clinic, where he presently is a Full Member in the Department of Immunology, Lerner Research Institute. A central aspect of Dr. Stuehr's research is focused on the structure, catalytic mechanisms, and regulation of redox enzymes. His laboratory currently investigates flavoheme enzymes such as NO synthases and NADPH oxidases as well as NO synthase-like heme proteins from bacteria. A second research interest concerns biological protein nitration, and his laboratory is currently studying the mechanisms and consequences of protein nitration that occur in mitochondria or other cell components as a consequence of inflammation or various autoimmune diseases.

to protect cells against oxidative damage. Regeneration of H_4B from its oxidized forms is particularly important in the biological system. The quininoid form of H_2B can be reduced by glutathione,[15] ascorbic acid,[16] or dihydropteridine reductase (DHPR), while the dihydro form of H_2B can be reduced by dihydrofolate reductase (DHFR).[17]

The oxidation rate of H_4B in aerobic solution depends on several factors, including pH, temperature, buffer, and reactant concentrations.[18] H_4B oxidation first generates quinonoid H_2B (qH_2B), which then rearranges to H_2B or forms pterin products with side-chain elimination depending on the reaction conditions.[12,19] Auto-oxidation of H_4B has been proposed to proceed by a free radical chain reaction initiated by reaction of O_2 and C4a of the pterin ring, with a cation H_4B radical forming as part of the chain reaction.[9] When N5 becomes protonated (monocation), H_4B is resistant to autoxidation, indicating that the electronic properties of biopterin are altered by protonation at N5. This is consistent with similar protection afforded by alkylation or acetylation[20] at N5 or replacement of N5 with a methylene.[21] Theoretical calculation in vacuo predicted that C4a of tetrahydropterin has the maximum electron density and that the adjacent nitrogen (N5) enhanced the reactivity of C4a. The low-energy π^* orbital of biopterin and large orbital coefficient at C4a are thought to explain this phenomenon. Slower reactivity of the N5-alkylated tetrahydropterins toward O_2 was suggested to be caused by steric hindrance of the 5-alkyl group in forming a presumed C4a-hydroperoxy intermediate.[21] Oxidation of tetrahydropterin under anaerobic conditions has been studied using chemical oxidizing agents such as ferricyanide or by electrochemical means.[22] Oxidation/reduction properties and midpoint potentials of H_4B and several related pterins have recently been studied using cyclic and square wave voltammetry.[23]

B. Structure of Pterin

Several pterin compounds have been crystallized: 5-formy-DMPH4,[24] 5-methyl-DMPH4,[25] 7,8-6MPH2,[26] and related 5,10-methylene-tetrahydrofolate.[27] The three tetrahydropterins all displayed a planar pyri-

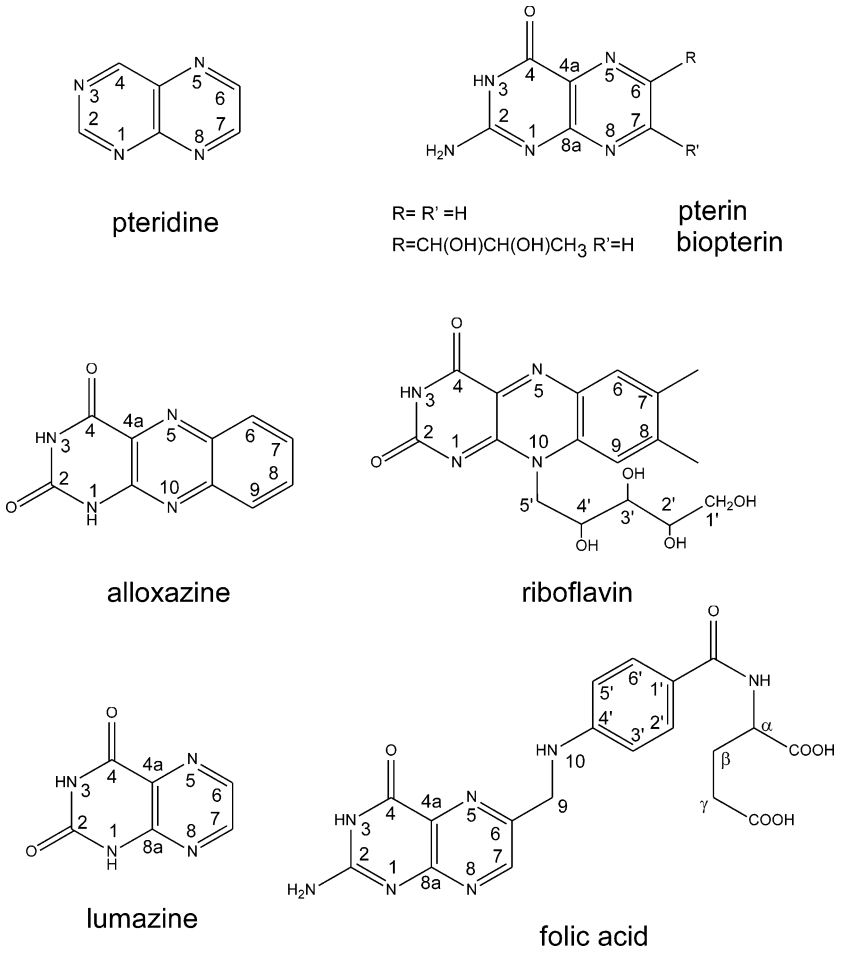

Figure 1. Chemical structures of some pteridines and alloxazines.

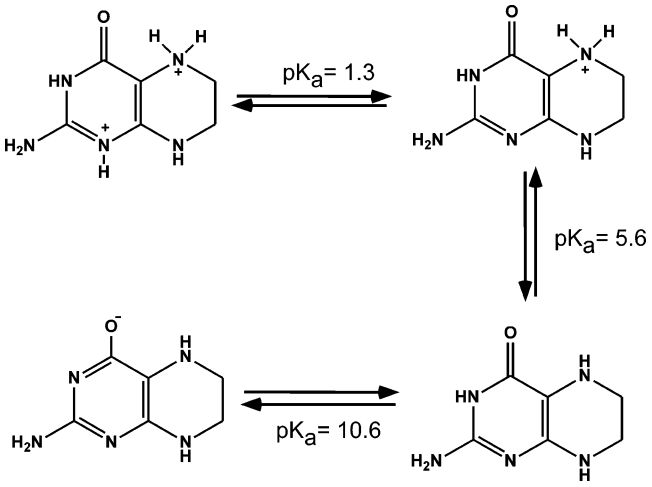

Figure 2. Protonation states of pterin.

midine ring with N8 and C7 coplanar to this ring, while C6 (sp^3) projects above the ring plain in a hemi-chair form (Figure 4). On the other hand, 7,8-6MPH2 displayed an essentially planar geometry throughout with π-electron delocalization into both pyrazine and pyrimidine rings. However, NMR studies indicated that the pyrazine ring of tetrahydropterin was in an equilibrium of two half-chair conformations in solution.[28−30] The C6-substituted tetrahydropterin analogues are interesting due to their, generally, being bound by biopterin-dependent enzymes, and the composition of the C6 side chain generally has a large influence on binding to enzyme.[31] Computational predictions of the H_4B structure were in agreement with the crystal structures regarding ring geometry but gave different results regarding the C6 side chain. Some studies suggested that the lowest energy conformation has the C6 side chain in the psuedo-equatorial position with a hydrogen bond formed between N(5)−H to the C(2′)−O.[32] Other models suggest the C6 side chain prefers the pseudoaxial position, with an understanding that the molecule is sufficiently flexible at C6 to prevent prediction of its geometry in an enzyme binding site.[33,34] An interesting difference regarding the dihydroxypropyl side chain of pterin is that the C1′ and C2′ hydroxyl groups were trans in the crystal structure but predicted to be cis in model calculations.[35] Recent NMR work on H_4B in neutral solution indicated that the C6 side chain curls back toward the pyrazine ring with its two hydroxyl groups in cis conformation.[36] Similar to those in solution, NOESY spectra of H_4B in NOS and AAH show that the dihydroxyl moiety is in the cis conformation.[35] However, in enzyme crystal structures the bound H_4B adopts both cis and trans conformations, with the C6 side chain only in the equatorial position (Figure 5). These differences indicate that solution structure studies may not accurately reflect the pterin binding geometry in enzymes.

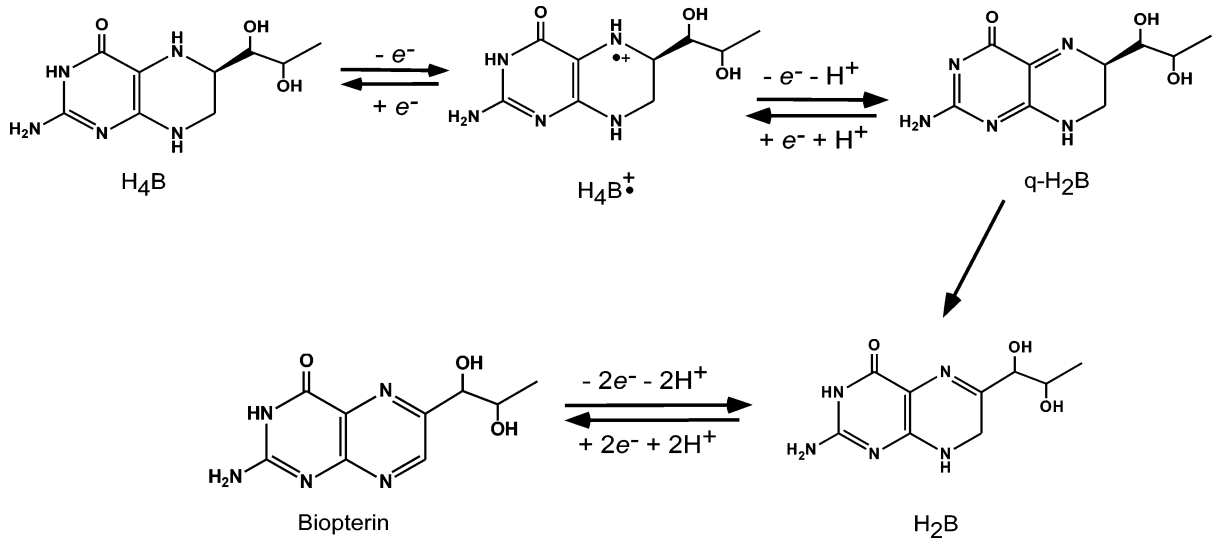

Figure 3. Redox states of H_4B.

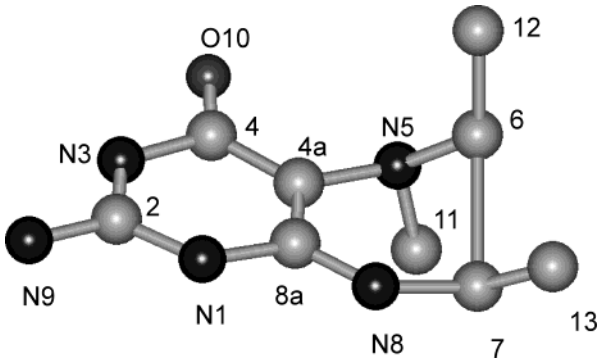

Figure 4. Crystal structure of 5-methyl-DMPH_4. Coordinates were taken from ref 25, and hydrogen atoms were omitted for clarity.

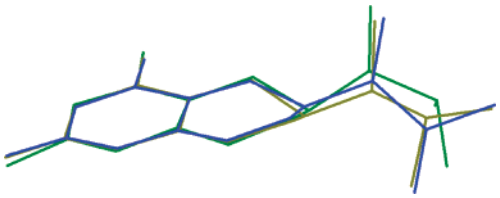

Figure 5. Superimposition of H_4B molecules bound in eNOS (yellow), iNOS (blue), and PheH (green).

C. Pterin Radical Generated from Chemical Reactions

Pterin radicals have been generated chemically in a variety of studies. A cation radical was generated by oxidizing tetrahydropterin (PH_4) or tetrahydrofolate (THF) with 1−1.3 equiv of H_2O_2 in a 6:1 mixture of CF_3COOH/CH_3OH.[37] The EPR spectrum in both cases showed a g tensor of ∼2.0 with unresolved hyperfine structure. The unpaired electron was predominantly localized at N5. Methyl group substitution at different ring positions gave a range of spin density (0.26−0.53)[38] at N5 consistent with computational results.[39] The spin density distribution was most sensitive to methyl substitution at N5 and N8 and least sensitive to substitution at the C6 position. Other methods used to generate and study the pterin cation radical include its reaction with superoxide in both aerobic and anaerobic conditions[13] and reaction with Cu(II) under N_2.[40]

Each biopterin or pterin cation radical generated in the various reactions under acidic conditions displayed a somewhat different EPR spectrum, possibly due to the different solvation and redox conditions. However, in each study it was concluded that the majority of unpaired electron spin density was located at N5. The cation radical was also relatively stable and had a very slow rate of dismutation[9,41] or reaction with O_2.[9,12,18] These cation radicals were considered to be protonated at N5, which was suggested to decrease the reactivity of the $H_4B^{\bullet+}$ species. In some cases UV or EPR spectra of neutral,[42] cationic,[42] and anionic[43] biopterin radicals were also reported. How the structure of the resulting radical differs from the parent structure is unknown. Conceivably, its solution structure could be predicted based on the EPR data and quantum chemical calculation, and this might broaden our understanding of H_4B radical formation in enzymes.

III. Biochemistry of H_4B

H_4B is a cofactor in enzymatic hydroxylation of aromatic rings, cleavage of glycerol−ether,[44] NO biosynthesis, and cyanide oxidation.[45] The closely related tetrahydropterins THF and molybdopterin also function as cofactors in various enzymes. Figure 6 compares different redox functions of H_4B or mTHF in three representative enzymes: NOS, phenylalanine hydroxylase (PheH), and thymidylate synthase (TS). In NOS, H_4B functions exclusively as a one-electron donor to a heme−dioxy enzyme intermediate, which will be discussed in greater detail in section IV. Enzyme reactions where H_4B functions formally as a two-electron donor occur in different ways. In the aromatic amino acid hydroxylases, the C4a atom of H_4B is thought to act as a nucleophile and react directly with O_2 to form a C4a−peroxy intermediate that, in conjunction with bound ferrous iron, hydroxylates aromatic substrates. In this monooxygenase reaction the two electrons originating from H_4B end up on the remaining C4a hydroxyl, which is released as water from the pterin. In the case of thymidylate synthase, which catalyzes reduction of C5 exocyclic methylene of dUMP, a direct hydride

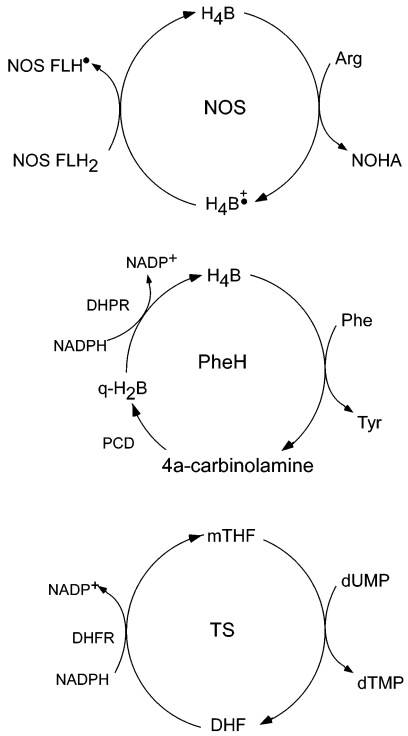

Figure 6. Redox functions of H_4B and mTHF in NOS, TS, and PheH.

transfer is thought to occur from C6 to the unsaturated substrate.[46] The three representative enzymes also differ in how they process their oxidized pterin cofactors (Figure 6). The H_4B radical remains bound in NOS and is subsequently reduced back to H_4B by an electron provided by the NOS reductase domain, such that it can participate in another round of oxygen activation within the same enzyme molecule. In this way NOS is similar to various molybdenum- and tungsten-containing enzymes that do not release their molybdopterin cofactor during multiple turnover catalysis. However, there is only indirect evidence that pterin redox transformations may occur in these enzymes during catalysis.[47] All other H_4B-dependent enzyme systems appear to release the oxidized cofactor after each catalytic turnover. The aromatic amino acid hydroxylases release C4a-hydroxy-pterin, whereas thymidylate synthase directly releases dihydrofolate (DHF). Distinct auxiliary enzyme systems also convert the oxidized cofactor back to H_4B. H_4B-dependent enzymes clearly differ in how bound H_4B is positioned in the protein with respect to substrates and to metal or heme prosthetic groups, if present. These aspects will be discussed in sections V and VI.

IV. Biopterin and NOS

A. Background and Mechanism of NO Synthesis

Thus far, NOS is the only enzyme where biopterin radical formation is clearly linked to its catalysis. Mammals express three main NOS isozymes [endothelial NOS (eNOS or NOS III), neuronal NOS (nNOS, NOS I), and inducible NOS (iNOS, NOS II)] along with several splice variants.[48−51] The NOS

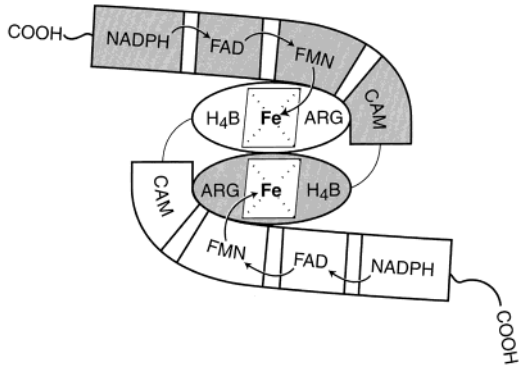

Figure 7. Electron-transfer pathway in dimeric NOS. CAM stands for a calmodulin binding sequence.

isozymes share ∼50−60% sequence homology and have similar structure. Each NOS polypepide is comprised of an N-terminal oxygenase domain that contains iron protoporphyrin IX (heme), H_4B, and a Arg binding site and a C-terminal reductase domain that contains flavin mononucleotide (FMN), flavin adenine dinucleotide (FAD), and a reduced nicotinamide adenine dinucleotide phosphate (NADPH) binding site (Figure 7). A calmodulin recognition sequence of approximately 30 residues is located between the oxygenase and reductase domains.

Electrons transfer from NADPH → FAD → FMN → Heme in NOS (Figure 7). Binding calmodulin triggers reduction of NOS ferric heme,[52] which is essential for O_2 binding and activation. Although NOS reductase domains are structurally and functionally similar to a family of NADP(H) utilizing flavoproteins that include cytochrome P450 reductase, they also contain two distinct sequence motifs that act in conjunction with calmodulin to regulate electron transfer.[53,54]

NOSs catalyze two sequential monooxygenase reactions: Arg is first hydroxylated to generate *N*-hydroxy-L-arginine (NOHA) as an enzyme-bound intermediate, which is further oxidized in a second reaction to generate nitric oxide (NO) and citrulline (Scheme 1). The first reaction consumes 1 mol of O_2 and 1 mol NADPH, while the second reaction consumes 1 mol of O_2 and 0.5 mol of NADPH. A mechanism for Arg hydroxylation has been modeled after cytochrome P450 monooxygenase chemistry[55] (Figure 8). Reduction of ferric heme enables O_2 binding and forms a ferrous−dioxy complex ($Fe^{II}O_2$ or $Fe^{III}O_2^-$).[56−59] This species obtains a second electron to form a presumed iron−peroxo species, which upon protonation and O−O bond scission generates water and a presumed iron−oxo speies (FeO) that is thought to hydroxylate a guanindino nitrogen of Arg.[60−64] The electron provided to ferric NOS heme comes exclusively from a FMN hydroquinone in the reductase domain,[53,64,65] whereas the electron provided to the $Fe^{II}O_2$ species can come from FMN hydroquinone[64] or H_4B.[7] Thus far only NOS species I ($Fe^{II}O_2$) has been observed to build up as a transient intermediate during single-turnover catalysis and has been characterized by a variety of spectroscopic methods.[56−59] NOS species II (peroxo−heme) was recently generated upon photoreduction of species I

Scheme 1

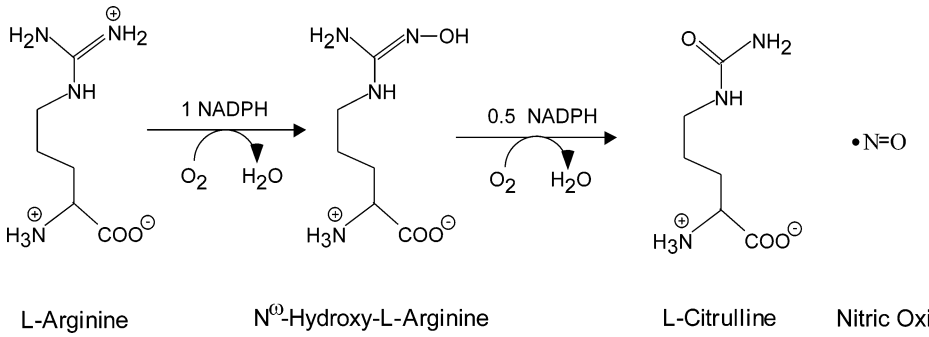

at cryogenic temperatures and was characterized by EPR and ENDOR spectroscopies.[66] Oxygen activation appears to follow a similar process in the second reaction of NO synthesis (NOHA oxidation), except that NOHA may be capable of providing an electron to the $Fe^{II}O_2$ species[63,67] as well as H_4B or the FMN hydroquinone.[7] After NOHA is oxidized the product NO binds to NOS ferric heme before leaving the pocket.[68,69] Transient ferric heme-NO complex formation and subsequent dissociation or reduction of this complex are fundamental kinetic parameters of NOS catalysis.[70,71]

B. H_4B Binding and NOS Activity

NOS was found to require H_4B as a consequence of its purification.[72,73] The affinity toward H_4B is such that NOS purified from animal tissues typically contains 0.2−0.5 H_4B per heme. H_4B binding to NOS is anticooperative, and binding H_4B to one subunit of the dimer (k_d = ∼nM) weakens the affinity for the binding to the partner subunit by at least an order of magnitude.[74] H_2B,[65,73] sepiapterin, 2′-deoxysepiapterin,[65,75,76] and 4-amino-H_4B,[31,76,77] all bind to NOS without supporting NO synthesis, consistent with a redox role for H_4B. Binding studies[75,78,79] that utilized radiolabeled H_4B indicate $k_{on} = 0.15-1.3 \times 10^6$ M^{-1} min^{-1} and $k_{off} = 0.06-3.2 \times 10^{-1}$ min^{-1}. Studies with various H_4B structural analogues indicate the following: (1) Compared to other H_4B-utilizing enzymes, NOSs display a higher affinity toward H_4B and a distinct hierarchy toward binding various pterins; (2) the tetrahydro redox state is not required for binding but is essential for supporting NO synthesis; (3) binding site occupancy by Arg or its structural analogues enhances binding affinity toward H_4B and vice versa; (4) pterin side-chain composition at C6 helps determine binding affinity but not catalysis.

In addition to substitutions at C6, H_4B analogues substituted at other ring positions can bind and support NO synthesis including 5MeH_4B, 2MeH_4B, 2-formyl-H_4B, 5-formyl-H_4B,[80] and 4-oxo-substituted tetrahydropterins.[81] Some tetrahydropterins bind but do not support catalysis. For example, 4-amino-H_4B has a higher affinity toward NOSs (K_d = 13 nM) compared with H_4B (K_d approximately 250 nM) but inhibits NO synthesis.[31,76,77] A recent NOS inhibitor design study was largely based on 4-amino-H_4B.[81,82]

H_4B binding site occupancy causes structural and electronic changes in NOS that are largely independent of pterin redox state. Structural effects include stabilizing the NOS dimer or promoting its formation,[83] protecting against proteolysis in a N-terminal hook structure,[79] slowing binding of CO[84] and other ligands to the heme,[85−87] and increasing Arg binding affinity.[76] Electronic effects on the heme include shifting the ferric iron spin state equilibrium toward high spin,[60,76,88] stabilizing six-coordinate forms of NOS ferrous−CO and ferrous−NO complexes[84,89] and altering the stability of the $Fe^{II}O_2$ complex.[56]

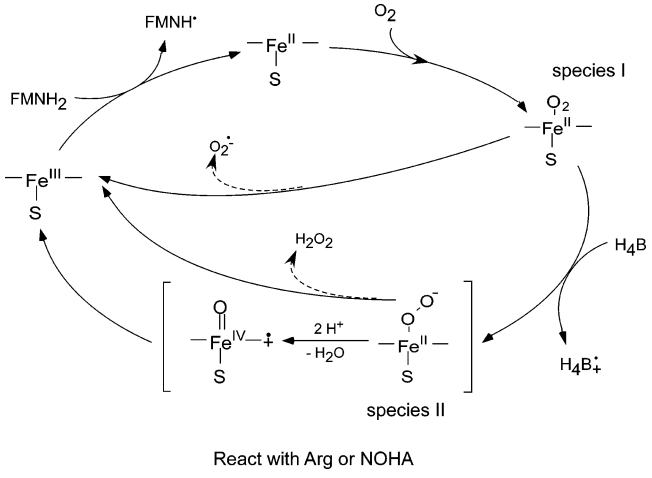

Figure 8. Oxygen processing steps at the NOS heme in relation to electron import, substrate oxidation, and superoxide or H_2O_2 release. The bracketed heme complexes have not been directly observed during catalysis.

C. Structure of NOS H_4B Binding Site

In recent years, the crystal structures have been determined for murine iNOSoxy,[90,91] human iNOSoxy,[92,93] bovine eNOSoxy,[94] human eNOSoxy,[93] and bacterial NOS-like protein.[95,96] These structures have defined similar dimeric states, subunit folds, cofactor binding sites, and substrate recognition for NOSs of different isozymes and species. A novel winged β-sheet with peripheral helices characterizes the NOS subunit fold.[90] Heme binds in a pocket between two roughly perpendicular β-sheets with Fe coordinated on the proximal side by a cysteine thiol. The substrate arginine and intermediate *N*-hydroxy-l-arginine (NOHA) bind with their guanidinium groups stacked against the distal face of the heme in a pocket formed by two β-strands of the winged sheet and the substrate binding helix α7a.

The NOS catalytic center, substrate binding site, active center channel, and pterin binding pocket are

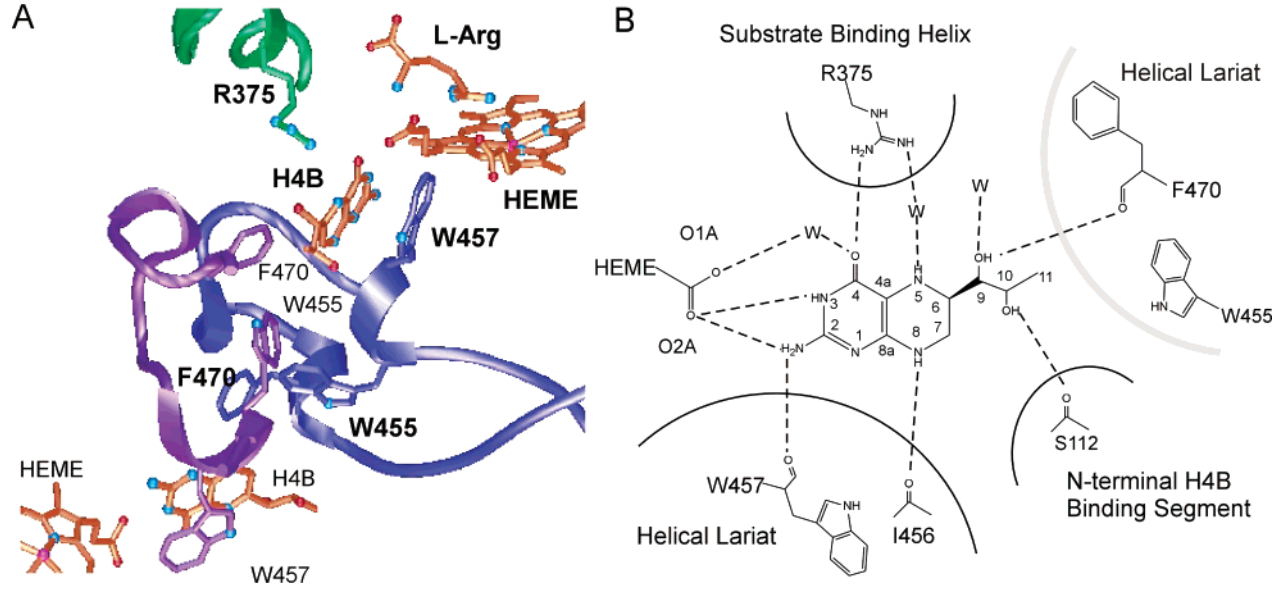

Figure 9. H_4B binding in an iNOSoxy dimer.

structured by subunit dimerization. Two H_4B molecules bind at the dimer interface and interact with two hydrophobic helical lariat structures. Two symmetric helical T regions frame the lariats and pterin binding sites. An N-terminal hairpin hook, important for stabillizing the dimer in some NOS proteins,[97] interacts with the H_4B dihydropropyl side chain and structures the opening to the substrate access channel. At the base of the N-terminal hooks, a zinc cation is tetrahedrally coordinated by four cyseine residues,[92,94,97] two supplied by each subunit. In the absence of zinc, two of the zinc-coordinating cysteines instead form an intersubunit disulfide bond.[91,92] Although dimerization impacts nearly all structural aspects of the NOS catalytic machinery, the two catalytic centers in the NOSoxy dimer appear to be chemically independent.[98−100]

The remote position of H_4B in NOS relative to the site of substrate binding and oxygen activation excluded the possibility that H_4B participates directly in either of the two substrate oxidation reactions. However, close structural coupling of a heme carboxylate with the pterin ring implies that the pterin is positioned well for electronic interactions with the heme. In the NOS pterin binding site, aromatic residues stack with the pterin ring whereas polar side-chain and main-chain groups provide edge-on hydrogen-bonding interactions to the pterin oxygens and nitrogens (Figure 9). In all NOSs a Trp (iNOS W457, eNOS W449) from one subunit and a Phe (iNOS F470, eNOS F462) from the other sandwich the pterin ring. A second Trp on the adjacent subunit (iNOS W455, eNOS W447) also buttresses the ring. The π-stacking interactions supplied by these aromatic residues are also preserved in iNOSoxy bound with inactive H_2B and 4-amino-H_4B.[101] An Arg (iNOS R375, eNOS R367) on the substrate binding helix (α7a) hydrogen bonds to pterin O4. Pterin N5 and N2 atoms hydrogen bond with peptide carbonyl groups on the helical lariat. The pterin site is well designed to facilitate electronic interaction between heme and H_4B by virtue of direct hydrogen bonds between a heme carboxylate and pterin N2 and N3. The same heme carboxylate group integrates H_4B binding with substrate binding by also forming hydrogen bonds to the substrate amino group (Figure 9b). Interactions of the H_4B dihydroxypropyl side chain include hydrogen bonds to Ser hydroxyl on the N-terminal hook and the peptide carbonyl of the same Phe that stacks with the pterin ring. Furthermore, Met114 and Trp84 (iNOS) on the N-terminal hook pack against the H_4B side chain and stabilize its conformation. NOS preferentially binds the 6(*R*) over the 6(*S*) pterin isomer.[65]

The protonation state of H_4B bound to NOS is currently unknown. On the basis of the binding of Arg in the pterin site when the high-affinity inhibitor S-ethyl-isothiourea (SEITU) occupies the substrate site, it has been suggested that H_4B binds in eNOS with N5 protonated and the ring positively charged.[94] However, a study investigating possible hydrogen-bonding interactions of H_4B and the inhibitor 4-amino-H_4B and their different pK_a values for N5 suggested that H_4B may bind in NOS as an uncharged species.[101] Electrostatic calculations indicate there is a negative potential at the NOS pterin in Arg-bound NOS (Figure 10). Because the protonation state likely impacts H_4B radical formation in NOS, it needs to be further investigated.

Overall, H_4B is an integral component of the NOS dimer interface and also provides interactions that structurally couple the heme center and substrate binding site to pterin recognition. Direct interactions between the heme carboxylate and the 3,4-amide of H_4B are consistent with H_4B donating electrons to the heme during catalysis. Furthermore, π-stacking interactions, an overall negative potential at the pterin site, and interaction of an Arg residue with pterin O4 may all facilitate H_4B radical formation in NOS (see below).

D. Biopterin Radical in NOS

A variety of studies suggested that H_4B may be redox active during NOS catalysis.[59,94,102] In particular, experiments that measured the extent of Arg

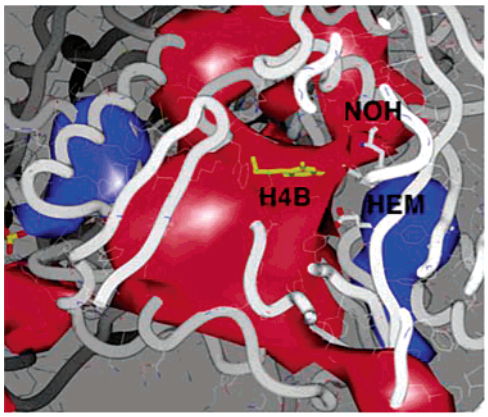

Figure 10. Electrostatic potential in the iNOSox H_4B site: negative potential (red contours at −12 kT/q), positive potential (blue contours at 12 kT/q). Contours were calculated with the Possion−Boltzmann equation (as implemented in SPOCK using an internal dielectric constant of 4 and external dielectric contstant of 80, 0.15 M ionic strength, and partial atomic charges).

hydroxylation by ferrous NOS under single-turnover conditions suggested that H_4B can provide the second electron required for O_2 activation.[59,103] H_4B was also found to speed disappearance of the $Fe^{II}O_2$ intermediate in NOS[56] and alter subsequent spectra collected during decay of the $Fe^{II}O_2$ intermediate at cryogenic temperatures.[59] This was followed by direct observation of a biopterin radical formed in single-turnover reactions catalyzed by iNOSoxy.[67] In this section we review the spectral and kinetic properties of the biopterin radical generated in NOS, discuss studies that examined how protein and pterin structure influence radical formation and stability, and discuss how and why biopterin radical formation is linked to other aspects of NOS catalysis.

E. Spectral Features of H_4B Radical in NOS

In single-turnover studies, ferrous NOSoxy or full-length NOS proteins that contain H_4B were mixed at 4, 10, or −25 °C with O_2-containing buffer to initiate the reaction. Radical formation was determined by recording EPR spectra of the samples at 4−150 K.[67,104] As shown in Figure 11, a radical signal with $g = \sim 2.0$, a peak-to-trough of ~40 G, and a resolved hyperfine structure was observed in enzyme reactions containing Arg or no substrate. No signal was observed with NOS samples that were H_4B free

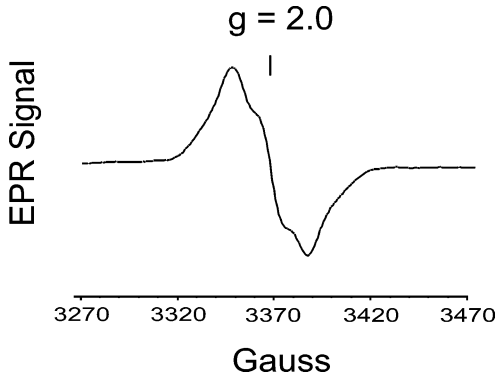

Figure 11. EPR spectrum of the H_4B radical formed during a NOS Arg hydroxylation reaction.

or contained H_2B in place of H_4B. The EPR spectrum of this radical was not temperature dependent in a range of 10−80 K, consistent with an organic radical. Substituting $^{15}N5-H_4B$ (^{15}N $I = {}^1/_2$) for H_4B (^{14}N $I = 1$) altered the hyperfine structure, consistent with spin density being mainly located on N5 of the biopterin ring, as observed for pterin cation radical generated in acidic solution.[37] In D_2O-enriched buffer the EPR hyperfine structure was altered, consistent with exchangeable protons being present at N5 in the bound H_4B. The somewhat wider spectrum of bound H_4B radical compared to that observed in solution was suggested to be due to either magnetic interactions of the radical ($I = {}^1/_2$) with ferric heme ($I = {}^5/_2$)[105] or strong hyperfine couplings with protons and/or nitrogens.[67]

Radical signals detected in experiments with nNOS and eNOS proteins all showed similar spectral features as for iNOS with somewhat different power saturation curves.[106,107] The similar spectra are consistent with the isozymes having very similar tertiary structure,[93] and the different power saturation profiles might reflect differences in how H_4B binding impacts protein structural stability and distribution among dynamic states for each NOS isozyme.[106]

Molybdopterin was implied to be structurally equivalent to the fully reduced tetrahydropterin oxidation state based on the stereochemistry at positions C6 and C7.[108] A molybdopterin radical with somewhat different hyperfine structure has been observed in certain bacterial aldehyde dehydrogenases following their purification.[47] Spin density was primarily located on N5 with magnetic interactions occurring with two protons. A simulation suggested that splitting is due to interaction with an exchangeable proton (H−N5) and one unexchangeable proton (H6),[47] similar to circumstances for the H_4B radical in solution or bound in NOS.

Although EPR data strongly support H_4B radical formation during NOS reactions, the protonation state of the radical has not been determined with certainty. Computer simulation of the hyperfine structure of the ^{15}N-containing radical was consistent with a protonated cation radical ($H_4B^{\bullet+}$).[106] However, recent reports from two different groups using similar computer simulations could not completely fit the experimental data, especially in the low- and high-field region.[107,109] It was also suggested that the H_4B radial in NOS may mimic the solution crystal structure based on a good agreement between calculated hyperfine splitting constants and geometric constraints.[106] In fact, solution studies of radical formation by isolated pterins indicates that ionization of the 3,4-amide group facilitates one-electron oxidation.[110] On the basis of these data, Crane et al. suggested that the NOS heme carboxylate may deprotonate the pterin 3,4-amide to aid radical generation and also shift negative charge to O4, to compensate positive Arg 375 (iNOS).[101] As the hyperfine interactions present in the EPR spectra are most sensitive to protons at N5, C6, and N8,[106] a shift of the N3 proton to the heme carboxylate to form a neutral $H_3B^{\bullet}$ radical may also be consistent with the observed data. Nevertheless, electrostatic calcula-

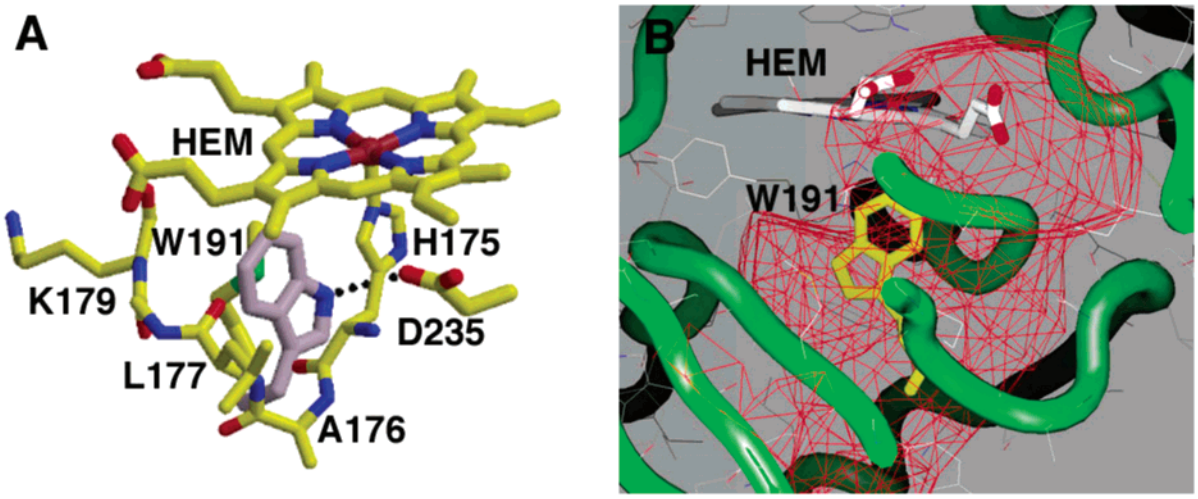

Figure 12. Yeast cytochrome *c* peroxidase site of radical cation formation (W191): (A) environment of Trp191 in cytochrome *c* peroxidase, (B) negative electrostatic potential surrounding Trp191 (red basket contours at −22 kT/q, calculated as in Figure 10).

tions indicate that the NOS pterin site has an overall negative potential (Figure 10). Thus, the heme carboxylate may only polarize the 3,4-amide and shift negative charge to O4 but not fully deprotonate the pterin. Thymidylate synthase, which oxidizes tetrahydrofolate to a radical in the last step of thymidine production, also recognizes the pterin 3,4-amide with a carboxylate group.[111,112] Negative potentials are also found in other enzymes at sites of radical cation formation. For example, cytochrome *c* peroxidase (CCP) forms a well-characterized indole cation radical at Trp191 during oxygen activation and compound I formation (Figure 12A).[113] Removal of this Trp191 by mutagenesis creates a cavity that will only bind positively charged indole derivatives.[114] As with the NOS pterin site, electrostatic calculations also predict that the CCP indole pocket also has a negative potential (albeit a much higher negative potential than in NOS) (Figure 12B).

F. Structural Influences on the NOS Biopterin Radical

Structural analogues 5MeH_4B and 6MPH4 also formed radicals in NOS during Arg hydroxylation reactions.[106] Because these tetrahydropterins also support NO synthesis,[80,115−117] the results strengthen the connection between pterin radical formation and catalysis in NOS. The 6MPH4 radical was found to have the same position and peak-to-trough distance as the H_4B radical, but hyperfine structure was no longer resolved.[106] For the 5MeH_4B radical, one group observed a broad spectrum with no resolved hyperfine structure[106] whereas another group observed hyperfine splitting for 5MeH_4B radical in NOS beyond what is seen for the H_4B radical.[109] The differences may relate to different solvent and mixing systems or to the different NOS isozymes used in the experiments.[118]

5MeH_4B and 6MPH4 may be able to form a radical in NOS and support NO synthesis because electronic characteristics at N3 of their pterin rings match those in H_4B.[39] N3 forms a direct hydrogen bond to the NOS heme propionate and is thought to be critical for electron transfer between H_4B and heme.[101] Indeed, the inability of 4-amino-H_4B to form a radical in NOS or support NO synthesis may be due to its ring having different electronic characteristics such that it is protonated when bound in NOS.[80]

Arg binding site occupancy is not required for H_4B radical formation in NOS.[67] The EPR spectrum of the radical is also identical in the presence or absence of Arg. Thus, the increase in ferric heme reduction potential brought on by Arg binding to the H_4B-saturated enzyme[119] is not required to drive H_4B electron transfer. H_4B radical formation in the absence of substrate likely allows NOS to generate H_2O_2 under this circumstance.[120] H_4B-bound nNOS recently was demonstrated to generate more H_2O_2 than H_4B-free nNOS in the presence of Arg.[121] Curiously, replacing Arg with NOHA resulted in very little H_4B radical accumulating in NOS during the single-turnover reaction, although NOS oxidized NOHA to NO plus citrulline in the same reaction.[67] This result has been interpreted to suggest that the H_4B radical does not form in the second step of NO synthesis[63,67] or that the radical forms and is then reduced such that it does not accumulate appreciably.[7,64,118,122,123] How structural analogues of Arg or NOHA might influence H_4B radical buildup has not been investigated.

Point mutation studies of NOS residues whose side chains interact with bound H_4B have indicated that most of them are important in preserving NO synthesis activity and in some cases also help stabilize NOS dimeric structure.[124−127] There have been different effects observed for mutations at a given residue depending on NOS isozyme identity (Table 1). Thus far only one of the residues (W457 in iNOS) has been studied with regard to its impact on the H_4B radical. The H_4B radical formed in Arg hydroxylation reactions catalyzed by W457A and W457F mutants had spectral characteristics that were identical to wild-type NOS.[128] This implied that the W457 mutations did not alter the spin density distribution or splitting interactions of the bound H_4B radical. How these mutations influenced kinetics of radical formation and decay is described in the next section.

Table 1. [a]

conserved residues (in murine iNOS numbering)	mutant	dimer (%) + H_4B + Arg	relative activity (%)	EC_{50} (μM)
	wt	**90−94**	**100**	**1.3**
R375	A (iNOS)	<10		
	L (eNOS)	N/A	59	
W455	A (iNOS)	<10		
	F (iNOS)	70	33	16
	Y (iNOS)	90	36	10
	L (nNOS)	28	<0.1	
W457	A (iNOS)	80	10	
	F (iNOS)	80	66	12
	L (nNOS)	15	<0.1	
	H (nNOS)	73	46	9
F470	A (iNOS)	<10		
	Y (iNOS)	90	75	3.3
	W (iNOS)	80	53	7.5
	L (nNOS)	43	<0.1	

[a] Data from refs 100, 125,and 168.

G. Kinetics of H_4B Radical Formation and Decay in NOS

Kinetics of H_4B radical buildup and decay have thus far only been reported in single-turnover reactions catalyzed by iNOSoxy.[67,104] When Arg hydroxylation reactions were run at 4 or 10 °C, the rate of H_4B radical formation was 11−15 s^{-1} and the rate of radical decay was 0.2−0.7 s^{-1} (Table 2). Reactions run with iNOSoxy that contained $5MeH_4B$[109] had a 4 times faster rate of pterin radical formation and a 3 times slower rate of radical decay compared to H_4B-containing enzyme (Table 2). Conversely, Arg hydroxylation reactions catalyzed by W457A and W457F iNOSoxy mutants had slower rates of H_4B radical formation than in wild type, while radical decay rates in these mutants were relatively faster (Table 2). In all cases, fitting indicated that practically all bound H_4B molecules had become oxidized to a radical during the single-turnover reactions. In all cases, H_4B radical decay in the NOS reactions proceeded much more slowly than decay of H_4B radicals formed in solution at neutral pH.[13,42] This was consistent with the slow off rate of H_4B from NOS enzymes (k_{off} = 3.2×10^{-1} min^{-1})[79] and indicated that NOS enzymes stabilize their bound H_4B radical, albeit to different extents. The diamagnetic product generated from H_4B radical decay was not identified in any of the studies but was suggested to be a further oxidized species such as H_2B. Together, these studies established the following: (i) rates of H_4B radical formation and decay are both influenced by pterin structure and by the surrounding iNOS protein residues; (ii) the speed of H_4B radical formation in iNOSoxy is related to the stability of the resulting radical. In fact, a plot of the available kinetic data indicated that the rate of H_4B radical formation is equal to the half-life of the resulting radical multiplied by a factor of 11.[109]

A crystal structure of $5MeH_4B$-bound iNOSoxy (Figure 13) showed that pterin ring orientation was essentially identical to that observed for bound H_4B with very little difference in surrounding protein structures as well.[109] There were some differences in the orientation of the C6 side chain and associated protein residues, which were suggested to help explain the poorer binding affinity of $5MeH_4B$. On the basis of the structural data the authors proposed that inherent electronic modifications of the N5-methyl substitution itself are primarily responsible for $5MeH_4B$ having faster radical formation and slower radical decay relative to H_4B. This is consistent with the methyl group providing added stability for a radical centered at N5.[129]

A crystal structure of the W457F iNOSoxy mutant (Figure 13) showed that the phenyl side chain of Phe457 was oriented similar to Trp and stacked in a near parallel manner with the biopterin ring.[130] Besides loss of one specific hydrogen-bonding interaction, there were no other differences in the W457F and wild-type structures. A crystal structure of the W547A iNOSoxy mutant (Figure 13) indicated discreet structural changes occurred near H_4B. The Ala substitution at position 457 creates a space that becomes filled by the guanidine side chain of Arg193. This structural change eliminates some hydrogen-bonding interactions and places the guanidine side chain up against the pterin ring in an approximately perpendicular orientation. Such placement of positive charge was suggested to destabilize the H_4B radical.[130]

The rates of H_4B radial decay were 0.7, 1.0, and 2.7 s^{-1} for wild-type, W457F, and W457A enzymes, respectively. If one assumes that a cation radical formed during the reaction,[106] these results are consistent with a model study on π−cation interactions of indole, phenol, or benzene to cation species.[131] Using ab initio methods, the binding energy for π-cation interacton was determined to be 32, 27, and 27 kcal/mol for indole (Trp), phenol (Tyr), and benzene (Phe), respectively.[132] Results from these quantum mechanical calculations also agreed with the trend obtained from semiempirical calculation. This type of interaction was predicted to predominate when the cation species and π system is within 4−6 Å, consistent with a crystal structure showing the parallel stacking distance of the biopterin ring and W457 is 3.6 Å. Furthermore, in an α-helical peptide

Table 2. Kinetic Parameters for Arg Hydroxylation Reactions[a]

iNOSoxy protein/ tetrahydrobiopterin	wt/H_4B	W457F/H_4B	W457A/H_4B	wt/$5MeH_4B$
$Fe^{II}O_2$ disappearance rate (s^{-1})	12.5 ± 0.2	6.5 ± 0.1	3.0 ± 0.1	34.7 ± 2.2
$Fe^{II}O_2$ disappearance rate + H_2B (s^{-1})	0.30 ± 0.08	0.37 ± 0.01	0.052 ± 0.003	0.30 ± 0.08
biopterin radical formation rate (s^{-1})	13	7.1	2.7	40
biopterin radical decay rate (s^{-1})	0.6	1.0	2.7	0.2
amount of biopterin radical formed per heme (%)	100	78	72	100
rate of NOHA formation (s^{-1})	9.2 ± 1.1	4.3 ± 1.2	2.6 ± 0.7	30 ± 4
NOHA produced per heme	0.61 ± 0.08	0.22 ± 0.1	0.15 ± 0.06	0.84 ± 0.07

[a] Data from refs 104, 109, and 128.

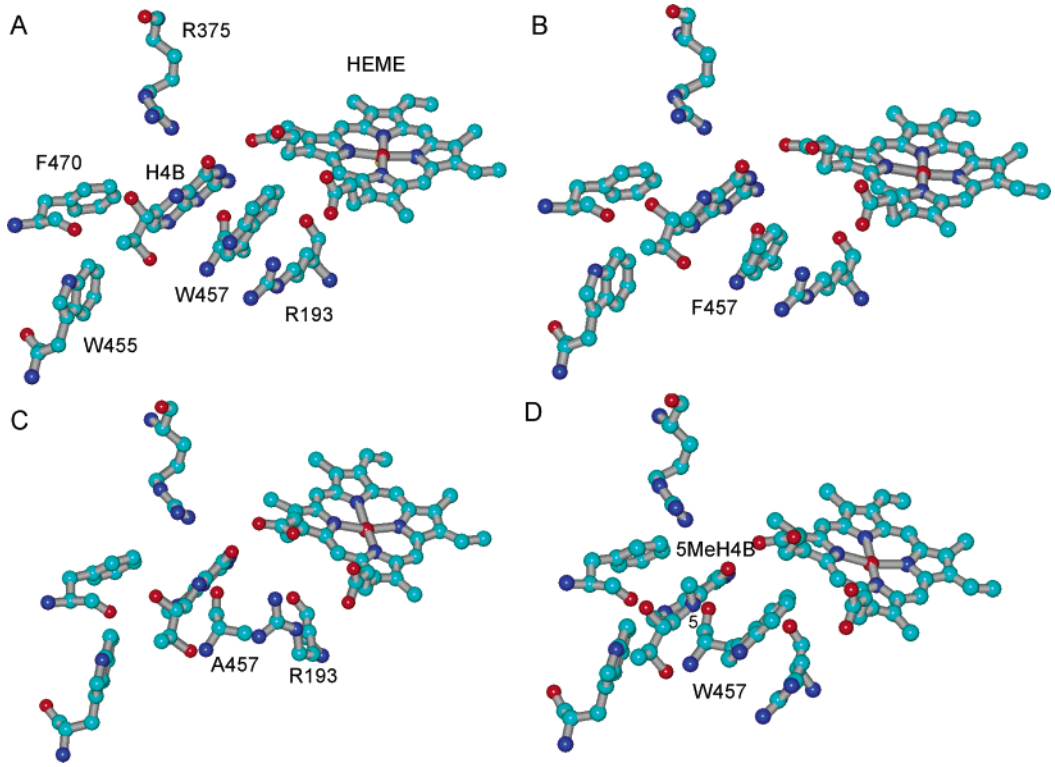

Figure 13. Biopterin binding sites of (A) H_4B-bound iNOSoxy, (B) H_4B-bound W457F iNOSoxy, (C) H_4B-bound W457A iNOSoxy, and (D) $5MeH_4B$-bound iNOSoxy.

model, interaction of Tyr with the cation species (Arg) was stronger than that of Phe[133] but significantly less than that predicted from theoretical calculation. Kappock and Caradona[5] also suggested that the stability of a pterin cation radical derives not so much from its protonated state as from its ability to restrict the lone pair of electrons on N5. This is consistent with the pterin hydrogen-bonding network being relatively well conserved in the W457 mutants such that the protonated state of the radical should be similar to that in wild-type NOS. Thus, the slower rate of H_4B radical formation observed in the W457 iNOSoxy mutants was not due to the disruption of electronic communication between pterin and heme or due to altered oxidation or protonation states of bound H_4B but rather due to a less than optimal stabilizing force provided by the protein environment to facilitate H_4B radical formation.

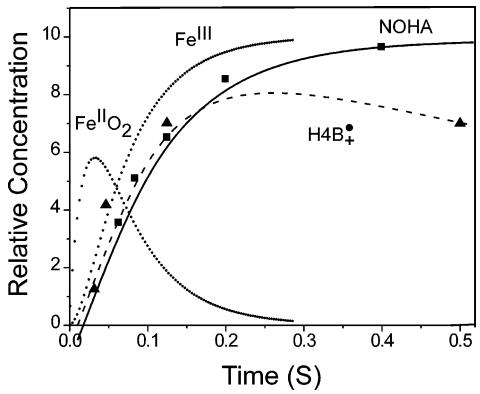

Figure 14. Kinetic relationships among heme $Fe^{II}O_2$ formation and decay, H_4B radical formation and decay, Arg hydroxylation, and heme Fe^{III} recovery in a single-turnover reaction catalyzed by H_4B−saturated iNOSoxy at 10 °C. Data are from ref 104.

H. Function of H_4B Radical Formation in NOS Catalysis

A role for H_4B radical formation has been established in the Arg hydroxylation reaction catalyzed by iNOSoxy. One-electron oxidation of H_4B occurs after a transient $Fe^{II}O_2$ intermediate forms in the reaction[104] (Figure 14). The electron from H_4B is thought to transfer to the enzyme $Fe^{II}O_2$ intermediate as part of its stepwise oxygen activation mechanism. This contention was based on (i) a close correlation between rates of H_4B radical formation, disappearance of the $Fe^{II}O_2$ intermediate, and buildup of the hydroxylated product in several different systems,[104,109,128] (ii) the relatively long lifetime of the $Fe^{II}O_2$ intermediate in NOSs that contained H_2B,[103,104,118,128,134] which is redox inactive and unable to support NO synthesis. Although H_4B is expected to function identically in all three NOS isozymes to reduce the $Fe^{II}O_2$ intermediate during Arg hydroxylation, kinetic data directly supporting this contention is not yet available for nNOS and eNOS. In those isozymes, an H_4B radical clearly forms during the Arg hydroxylation reaction,[106] but its kinetics of formation and decay have not been studied in relation to $Fe^{II}O_2$ disappearance rates[103] or rates of product formation.[135]

H_4B radical formation and associated electron transfer appears to be responsible for keeping NOS heme reduction well-coupled to Arg hydroxylation.[7,120] In the absence of H_4B, NOS heme reduction was greatly uncoupled from substrate oxidation in both conventional and single-turnover reactions.[60,64] NOS ferric heme is only reduced by the attached

Scheme 2

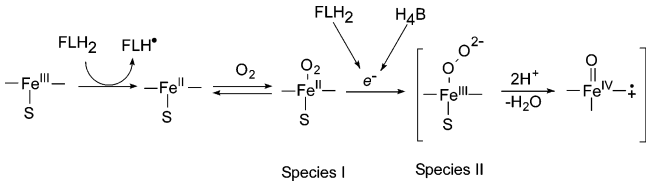

flavoprotein domain (Scheme 2), whereas the $Fe^{II}O_2$ intermediate may accept electrons from either the flavoprotein or H_4B[59,64] (Scheme 2). Due to relatively slow ferric heme reduction rates in NOS,[134] the enzyme appears to use H_4B as a kinetically preferred source of the electron required to reduce the $Fe^{II}O_2$ intermediate. This function appears to be important because of a competing reaction that involves nonproductive decay of the $Fe^{II}O_2$ intermediate[7,104] (Figure 15). Indeed, slower H_4B radical formation in Arg single-turnover reactions catalyzed by iNOSoxy is associated with a proportionally lower product yield,[128] whereas faster rates of radical formation are associated with increased product yield.[109]

Evidence indicates that the bound H_4B radical formed in NOS during Arg hydroxylation must be reduced back to H_4B before NOS continues on to the second step of NO synthesis.[104,118,123] Thus, stabilizing the bound H_4B radical is a fundamental facet of NOS catalysis. Stoichiometric considerations imply that the electron derives from NADPH and is provided by the NOS reductase domain. The available kinetic data is consistent with this possibility: The rate of ferric heme reduction in iNOS was determined to be $1-2\ s^{-1}$ at 10 °C,[134] which represents an electron transfer by the reductase domain that would be sufficiently fast to reduce the H_4B radical before it decays (decay rate was $0.2-0.7\ s^{-1}$ at 4 or 10 °C).[67,104] The mechanism governing reduction of the H_4B radical in NOS remains to be established.

Much less H_4B radical buildup has been observed (approximately 0.03 per heme) in single-turnover studies of the second reaction of NO synthesis.[67] Thus, its role as an electron source in this step remains to be definitively established. Some indirect evidence supporting H_4B radical formation is available.[118,123,136] In particular, iNOSoxy W457 mutants that catalyzed slower H_4B radical formation, slower $Fe^{II}O_2$ disappearance, and a lower product yield in Arg hydroxylation reactions also catalyzed slower $Fe^{II}O_2$ disappearance and lower product yield in NOHA single-turnover reactions.[136] Related studies showed that NOHA is poorly oxidized in single-turnover reactions catalyzed by H_2B-containing NOSoxy enzymes.[136] In addition, crystallographic data and single-turnover studies suggested that NOHA is unable to reduce the NOS $Fe^{II}O_2$ intermediate.[101,123,136] These are also consistent with H_4B having a redox function in the second step of NO synthesis. One mechanism put forward to explain how H_4B could act as an electron donor in the NOHA reaction despite minor H_4B radical buildup has the H_4B radical forming and then becoming reduced at a later point in the reaction[6,7,64,123,136] (Figure 16). A sequential electron-donor electron-acceptor function for H_4B is attractive because it has H_4B acting similarly in both steps of NO synthesis and helps to explain why H_4B is absolutely required by NOS to generate NO from NOHA and why NOS generates nitroxyl (NO^-) from NOHA in the absence of H_4B.[64]

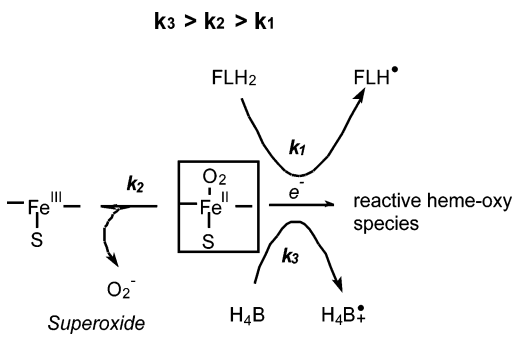

Figure 15. Partitioning of the NOS $Fe^{II}O_2$ intermediate by either reductive or oxidative pathways.

V. H_4B Binding and Function in AAH Enzymes

AAHs are non-heme iron monooxygenase enzymes that are responsible for hydroxylating the aromatic rings of Phe, Tyr, and Trp. Their reaction mechanisms have been extensively studied and show similar features.[3] H_4B functions in AAH differently than in NOS in three fundamental ways: H_4B becomes oxidized by two electrons rather than by one electron, participates directly in oxygen activation, and is released from the enzyme after each catalytic cycle. Oxygen activation appears to involve O_2 binding to the 4a position of H_4B and requires the closely associated iron atom. The exact hydroxylating species is still a matter of debate, but various evidence has implicated a 4a-peroxo−pterin or a high valence iron−oxo species.[3,5,137−141]

Although the quaternary structures of AAH are quite different, their catalytic domains are well conserved, consistent with their sharing a common catalytic mechanism. Crystal structures of PheH,[142,143] TyrH,[144] and TrpH[145] revealed similar catalytic domain structures for the three classes of hydroxylases. These enzymes all fold in a basket-like arrangement of α-helices and β-loops that generate a deep cleft at the center of the molecule for binding non-heme iron, H_4B, and substrate. At the base of the cleft, the iron atom (Fe^{II} or Fe^{III}) is coordinated to two His residues that project from consecutive turns of the same α-helix and a Glu extending from the base of a second helix perpendicular to the first (Figure 17, 1J8T and 1KWO). A variable number of water molecules complete the iron coordination geometry depending on iron redox state and the presence of cofactors and/or substrate (Figure 17). The ferric iron in TyrH has a square pyramidal structure with coordination to His331 (numbering in rat TyrH), His 336, Glu 376, and two water molecules. The structure of ferric PheH is similar to TyrH except that an additional water molecule occupies the sixth coordination site of the iron (His285, His 290, Glu330, and three water molecules) to form an octahedral geometry. Ferric and ferrous enzyme forms have a different geometry in the active site,[143] suggesting redox-based conformational change may contribute to the driving force for the reaction.

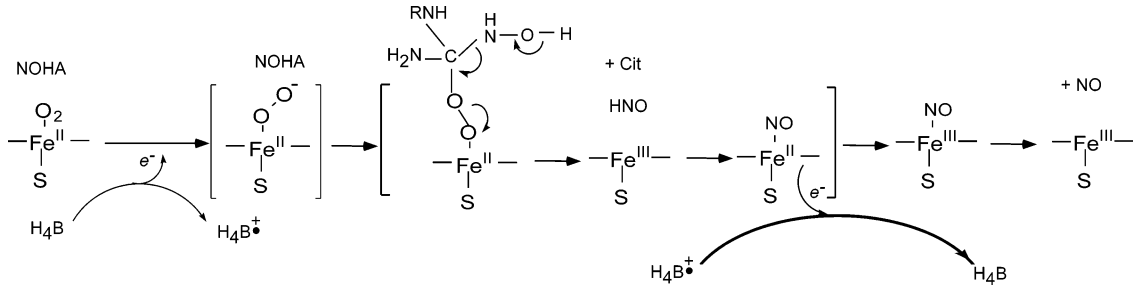

Figure 16. Proposed dual-redox function for H_4B function in NOHA oxidation by NOS. H_4B first donates an electron to the $Fe^{II}O_2$ intermediate to enable formation of the ultimate heme-based oxidant. Then a subsequent heme intermediate that forms in the reaction sequence transfers an electron back to the H_4B radical to regenerate fully reduced H_4B.

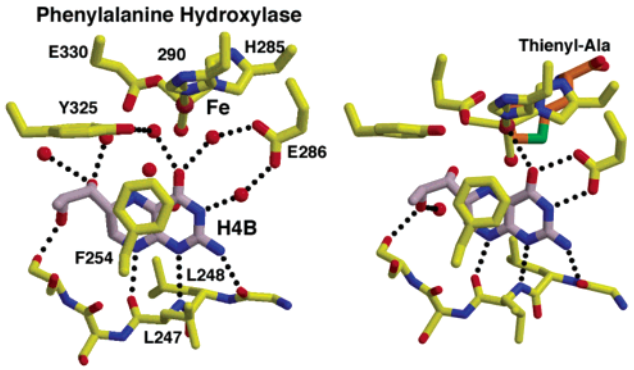

Figure 17. H_4B binding site in PheH.

The mode of biopterin binding depends on the redox state of iron and the presence of substrate. However, in all cases 7,8-H_2B binds along the edge of the active center cleft in close proximity of iron. The pterin ring stacks against a Phe, with an interaction reminiscent of how the NOS pterin stacks with Trp. In TyrH this Phe was found to be hydroxylated.[144] The pterin directs O4 toward the non-heme iron, whereas the other edge of the pterin interacts with an extended β-strand near the top of the cleft that supplies a conserved carbonyl for hydrogen bonding to pterin N8. In TyrH and PheH a Leu side chain from the preceding residue stacks against the reduced pteridine ring, whereas in TrpH this residue is a Tyr. The pterin side chain participates in somewhat different interactions in the three hydroxylase classes. In PheH the extended strand containing the ring-stacking Leu also provides a Ser for hydrogen bonding to the terminal pterin hydroxyl group, whereas in TrpH this hydroxyl abuts a Pro. In TyrH bound with 7,8-dihydrobiopterin the pterin side-chain orientation differs with the terminal hydroxyl directed toward the non-heme iron instead of the peripheral extended strand.

Human PheH is the only enzyme where a structure has been determined with H_4B bound[142] and the reduced pterin binding mode depends highly on the presence of a substrate analog.[143] In the absence of substrate H_4B binds much like H_2B, but when the substrate analogue 3-(2-thienyl)-L-alanine binds H_4B shifts in the pocket to allow interactions between a glutamate carboxylate and the pterin 3,4-amide and between the iron and pterin O4 (Figure 17). Other larger changes compact the protein and generate a substrate binding pocket adjacent to the iron site. Water molecules that bridged interactions between the glutamate and 3,4-amide in the absence of substrate are excluded from the active center, which has become generally desolvated. The structural data was consistent with biochemical experiments that showed activation of PheH by substrate is highly cooperative and always accompanied by alterations in tertiary structure[146] and also was consistent with electrochemical measurements with PheH that showed binding substrate or biopterin (H_2B) decreased the ferric iron midpoint potential from +207 to +123 or +110 mV, respectively.[147]

It is interesting to note that in the substrate−cofactor−iron ternary complex the pterin of PheH has similar interactions with the protein as does the pterin in NOS. Aromatic amino acids stacking with the pterin ring is a conserved theme, as is the carboxylate interaction with the 3,4-amide. These aromatic π-stacking interactions are observed in enzymes (Phe300 in TryH and Phe254 in human PheH). Mutation of Phe254 to Ile in PheH caused distortion of the important cofactor π-stacking interactions.[148] The stacking distance between the pterin and Phe is 3.6[149] to 3.7[150] Å, similar to that in iNOSoxy. In the absence of substrate, biopterin adopts an expected semi-chair conformation in the enzyme with a C4a to iron distance of 5.9 Å.[142,144] However, substrate analogue binding to PheH−Fe(II)−H_4B shortened the distance between the iron and C4a, C4, and N5 and brings O4 into the iron coordination sphere (3.3 Å),[143] suggesting a means by which conformational change could facilitate formation of a putative Fe^{II}−O−O−H_4B intermediate. The conservation of the pterin 3,4-amide interaction with a carboxylate base (see also description of molybdopterin enzymes to follow) suggests that deprotonation of the 3,4-amide could be generally important for producing oxidized pterin states during catalysis. A recent mechanistic study using hybrid density functional theory suggested formation of a C(4a)−O bond is the rate-limiting step in the formation of Fe^{IV}=O.[151]

VI. Molybdopterin Radicals in Molybdenum and Tungsten Enzymes

In addition to the NOS proteins, a pterin radical has also been observed in bacterial aldehyde dehydrogenases (ADHs). ADHs belong to a large and diverse class of enzymes that contain tetrahydropteridine rings modified to bind either molybdenum or tungsten.[108,152,153] The pterin cofactor common to

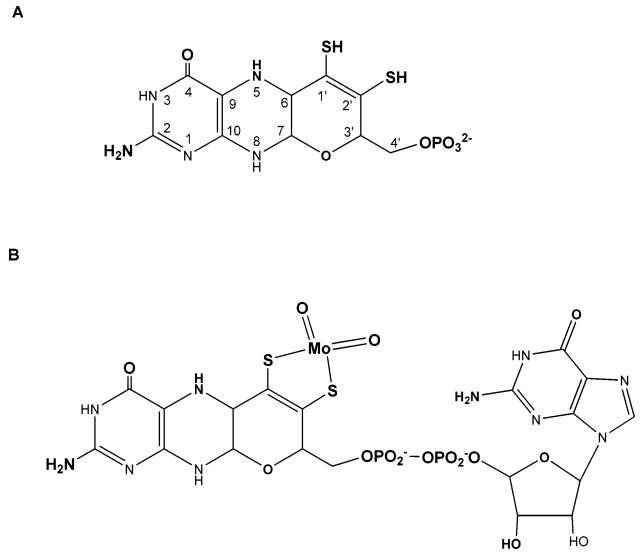

Figure 18. Structures of the molybdopterin cofactor: (A) organic component, (B) molybdopterin guanine dinucleotide form as found in DMSO reductase.

all of these enzymes consists of a tricyclic pyranopterin with a *cis*-dithiolene in the pyran ring for coordinating either Mo or W (Figure 18). Among the molybdopterin (MPT) enzymes the Mo/W coordination sphere forms from either one or two coordinating MPT cofactors, which can be further derivatized with nucleotide phosphates, such as guanosine mononucleotide (GMP). The MPT enzymes usually catalyze oxo transfers to or from substrates with subsequent two-electron oxidation or reduction of Mo(VI/IV). The catalytic cycle is completed by electron transfer involving the Mo center and additional redox cofactors (FeS clusters, flavins, or hemes) contained within the MPT proteins or partner proteins. The close structural coupling of single-electron donors/acceptors (primarily FeS clusters) adjacent to the pteridine ring suggests involvement of pterin radical states in redox recycling of the Mo center. In fact, EPR spectroscopy on ADHs indicates not only the presence of a stable pterin radical, but also electronic interaction between this radical and a closely associated Fe_2S_2 cluster.[47]

There are four families of MPT enzymes. Although members of a given family are structurally homologous, there is little sequence similarity or structural homology between any two families.[152] Furthermore, within a family, the enzyme active sites and reactions catalyzed therein can be quite diverse despite some conservation of MPT environment and geometry. The four MPT families are named for their representative members: (1) dimethylsufoxide (DMSO) reductase, (2) xanthine oxidase (XO), (3) sulfite oxidase (SOX), and (4) aldehyde ferredoxin reductase (AOR). In all families, MPT cofactors are bound in the center of the protein, usually at an interface between domains or subunits. Characteristically, a long funnel or channel leads to the Mo coordination sphere and site of catalysis. A number of excellent reviews have summarized the structure and chemisry of MPT proteins.[154,155] Below we describe general characteristics of pterin environments in four MPT families and provide one family member as an example. We will focus on the tetrahydropteridine ring common with NOS and consider the possibility of radical formation during intramolecular electron transfer (ET) to or from the Mo/W center. It should be noted that a given family can contain enzymes that function as either reductants or oxidants of their redox partners (for example, sulfite oxidase and assimilatory nitrate reductases).

A. The DMSO Reductase Family

In addition to DMSO reductase (DMR),[156−158] this family includes dissimilatory nitrate reductase (DNR),[159] formate dehydrogenase H (FDH),[160] and formate dehydrogenase N (FDN).[161] DMR and DNR function as oxidants of their redox partners, whereas FDH and FDR function as reductants. The protein or subunits responsible for binding MPT in these proteins have a 4- or 5-domain $\alpha + \beta$ structure that arranges around two molybdopterin guanine dinucleotide (MGD) cofactors (named the P- and Q-pterin). In the α subunit of the membrane protein formate dehydrogenase N (Figure 19A, 1KQF) one MGD is within 6.0 Å of an Fe_4S_4 cluster which begins an electron-transfer pathway of cofactors from the α subunit through the membrane to the periplasm. A conserved lysine residue bridges hydrogen-bonding interactions between a cluster cubane sulfur and N2 of the pterin ring in FDH (1AA6), FDN (1KQF), and DNR (2NAP) (Figure 19, 1KQF). The pterin ring coupled to the FeS cluster is sequestered from solvent with a Phe stacking on one side of the pterin and main chain buttressing the other. An Arg hydrogen bonds to N5 as well as N5 and O4 of the other MPT cofactor, whereas backbone carbonyl oxygens hydrogen bond to pterin N2 and N8, as in NOS. The polarity and nature of the immediate environment surrounding the P- and Q-pterins varies throughout the family, making it difficult to draw conclusions as to structural features that might facilitate electron transfer to one pterin over the other. For example, in formate dehydrogenase H, the pterin furthest from the cluster is in the most polar environment, being partially exposed to solvent, whereas in nitrate reductase the pterin furthest from the FeS cluster is in a more nonpolar environment with extensive aromatic stacking interactions with the protein. This difference may reflect the fact that FDH reduces redox partners whereas DNR oxidizes them. DMSO reductase does not contain an additional redox cofactor, and neither of the pterins stack with protein aromatic residues. If pterin radical states are involved in ET, protein environment may tune the pterin potential to be appropriate for the potentials of the Mo centers and redox partners. Radical formation on the pterin ring has not yet been detected in any member of this family, although the close association of the FeS clusters with one of the pterins suggests pterin involvement in electron-transfer reactions.

B. The XO Family

In additon to xanthine oxidase/dehydrogenase (1FIQ/1FO4),[162] this family includes aldehyde oxidase

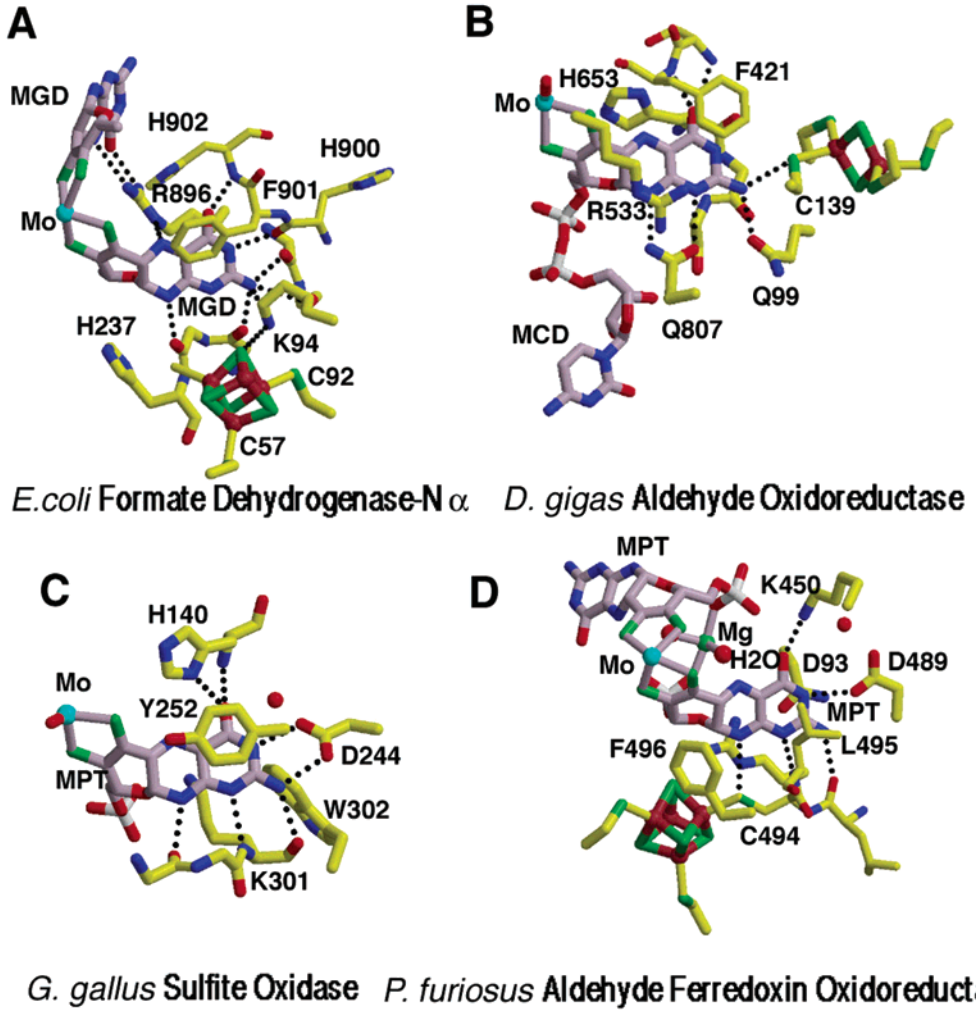

Figure 19. Pterin environments in four structural families of molybdenum and tungsten enzymes. (A) DMSO Reductase family represented by *E. coli* formate dehydrogenase-N (PDB code 1KQF). Two molybdopterin guanine dinucleotides each provide two thiolene ligands to coordinate Mo (guanosine groups not shown). (B) The Xanthine Oxidase family represented by *D. gigas* aldehyde oxidoreductase (1HLR). One molybdopterin cytidine dinucleotide coordinates the Mo. (C) Sulfite Oxidase family represented by chicken liver sulfite oxidase (1SOX). One molybdopterin coordinates the Mo. (D) Aldehyde Ferredoxin Oxidoreductase family represented by *P. furiosus* aldehyde ferredoxin oxidoreductase (1AOR). Two molybdopterins coordinate the W.

(1HLR, 1DGJ),[163,164] aldehyde dehydrogenase, and CO dehydrogenase (1QJ2).[165] The ADH enzymes within which pterin radicals have been observed[47] belong to this family and share 32−55% sequence similarity with the *D. gigas* aldehyde oxidase, whose structure is known (1HLR).[163,164] The ADH enzymes contain a single molybdopterin cytosine dinucleotide (MCD), two Fe_2S_2 clusters, and in the case of the ADHs a flavin cofactor. In *D. gigas* aldehyde oxidase the MCD resides in a single domain that can be considered as being composed of four subdomains; the two FeS clusters are bound by a ferredoxin-like and 4-helix bundle domain, respectively. As with the DMSO reductase family, the pterin closely associates with the second Fe_2S_2 cluster and hydrogen bonds to a cluster ligating cysteine with N2 (Figure 19B, 1HLR). A Phe and Arg guanidinium stack with the pterin, on one side. Compared to the DMSO reductase family, the peptide carbonyls that hydrogen bond to pterin N2 and N8 are replaced by Gln side chains. As isolated, the ADH enzymes contain a Mo(VI) trihydropterin radical.[47] Given the negative reduction potentials of the oxidizing FeS clusters the XO family,[166] the Mo(VI) trihydropterin state in isolated ADH indicates that the trihydropterin radical has a relatively low reduction potential.

C. The SOX Family

The SOX family contains human sulfite oxidase[154] and the assimilatory nitrate reductases from higher plants. Sulfite oxidase has a mixed $\alpha + \beta$ structure with three domains. Domain I resembles cytochrome b_5 and binds heme. Domain II primarily binds the single MPT cofactor (with no nucleotide derivatization). A long flexible linker between Domain I and Domain II is not entirely discernible in the structure. The 3,4-amide end of the pterin ring projects toward the proteins surface but is sequestered by an Asp residue that recognizes pterin N2 and N3 similarly to how the heme carboxylate in NOS binds H_4B (Figure 19C, 1SOX). Curiously, the heme redox partner in domain I is over 30 Å from the pterin ring. However, the length and flexibility in the linker between domains I and II suggest that domain I may move in solution to better interact with the pterin.[153] The closest contact to the pterin and domain I would

involve domain I binding on the surface adjacent to the Asp that interacts with the pterin 3,4-amide. As with the other families, an aromatic residue (Tyr) stacks on one side of the pterin and backbone peptide groups hydrogen bond to pterin N1, N2, and N8.

D. The AOR Family

The tungsten-containing aldehyde ferrodoxin oxidoreductase (AOR) from the extreme thermophile *P. furiosus* was the first MPT protein to have its structure determined (1AOR). AOR is a dimer with each subunit consisting of three domains. At the domain interface two molybdopterins coordinate W via four dithiolene sulfurs as in the DMSO reductase family. One of the pterin rings is closely coupled to an Fe_4S_4 cluster by a direct hydrogen bond between pterin N8 and a cluster-ligating cysteine sulfur (Figure 19D). In the structure of *P. furiosus* formaldehyde ferrodoxin oxidoreductase (FOR),[167] the redox partner ferredoxin interacts on the protein surface adjacent to the Fe_4S_4 cluster (1B25). Both of these enzymes oxidize ferredoxin and could generate pterin radicals in this process. Like the SOX family and NOS, a carboxylate hydrogen bonds to N3. Both pterin sites in AOR and FOR are considerably polar, and neither enzyme supplies an aromatic residue for stacking with a pterin ring, Instead, a Mg^{2+} cation coordinated by the pterin phosphate group contacts both rings and, in FOR, pterin O4 coordinates a Ca^{2+} cation. In general, there are a number of charged groups (Arg and Lys) surrounding both pterins in these structures with main chain providing hydrogen bonds to N1, N2, and N5.

E. Pterin Environments in Mo/W Enzymes and NOS

In general, NOS and the four MPT families share common structural features at their pterin sites, although no one characteristic is conserved by all members of all families. Coordination of the fused pyran ring to Mo/W alters interactions of the pterin side chain compared to NOS, but the bicyclic tetrahydropteridine ring has similar geometries in the two classes of enzymes. In NOS and the MPT proteins the pterins are bound at interfaces between domains or subunits by irregular β-structure or turn regions that allow main-chain as well as side-chain interactions to pterin. Most intriguing perhaps is that NOS and a large number of MPT enzymes have a redox partner in close association with the 3,4-amide of the pteridine ring. Either a direct or bridged hydrogen bond connects the pterin ring to a heme (NOS) or an iron−sulfur cluster (MPT, families 1, 2, and 4). This suggests that the pterin ring does participate in electron transfer to the redox partner, although whether this process always involves radical formation (as in NOS and ADH) or electron-tunneling (superexchange) through the pterin remains to be established. The NOS and MPT proteins also often provide an aromatic ring to stack with the pterin in approximately the same position as the NOS Trp (iNOS W457). This interaction may be simply convenient for binding and positioning the pterin or could modulate pterin redox properties. It will be interesting to learn how redox reactivity of pterins in these enzymes differs depending on aromatic stacking interactions. One clear difference between pterin sites in NOS and the MPT proteins are that the latter are much more buried. The NOS pterin ring exposes the O4, N5 edge to solvent in the substrate access channel, whereas in most of the MPT proteins the rings are completely sequestered. Interestingly, in the MPT proteins there is often an ionizable residue (often a His) close to the O4, N5 edge of the pterin. If radicals do form on the pterin ring, such residues may couple protonation states to oxidation states. The high metal oxidation states, large number of ionizable groups, and buried nature of these sites complicates analysis of the electrostatic potentials surrounding the MPT cofactors, which may be a principle determinant governing pterin oxidation. Because the accepting or donating ET cofactors of the MPT proteins generally have low reduction potentials, for pterin radicals to form they must have relatively low reduction potentials relative to H_3B in NOS. The structural diversity composing MPT sites may reflect the necessity of tuning the pterin potentials to match those of the enzyme substrates and redox partners. Given the wealth of structural information available on the MPT proteins, more experiments investigating the participation of the MPT pteridine rings in electron transfer will significantly increase our understanding of how pterin reactivity is controlled.

VII. Abbreviations

$5MeH_4B$	5-methyl-6,7,8-trihydrobiopterin
6MPH4	6-methyl-5,6,7,8-tetrahydropterin
AAH	aromatic amino acid hydroxylase
ADH	aldehyde dehydrogenase
AOR	aldehyde ferrodoxin oxidoreductase
CaM	calmodulin
CCP	cytochrome *c* peroxidase
DHF	7,8-dihydrofolate
DHFR	dihydrofolate reductase, EC 1.5.1.3
DHPR	dihydropteridine reductase, EC 1.6.99.7
DMPH4	dimethyl-5,6,7,8-tetrahydropterin
DMSO	dimethylsufoxide
DNR	dissimilatory nitrate reductase
dTMP	deoxythymidine-5′-monophosphate
DTT	dithiothreitol
dUMP	2′-deoxyuridine-5′-monophosphate
FAD	flavin adenine dinucleotide
FDH	formate dehydrogenase
FMN	flavin mononucleotide
FOR	ferrodoxin oxidoreductase
EPR	electron paramagnetic resonance, ESR
H_2B	7,8-dihydrobiopterin
H_4B	(6*R*)-5,6,7,8-tetrahydrobiopterin
Heme	protoporphyrin IX
K_a	acid ionization constant
K_d	dissociation constant
MCD	molybdopterin cytosine dinucleotide
MGD	molybdopterin guanine dinucleotide
MPT	molybdopterin
mTHF	5,10-methylene tetrahydrofolate
NADPH	ncotinamide adenine dinucleotide phosphate hydrogen
NMR	nuclear magnetic resonance
NOHA	*N*-hydroxy-L-arginine

NOS	nitric oxide synthase, EC 1.14.13.39
PCD	pterin 4a-carbinolamine dehydratase, EC 4.2.1.96
PheH	phenylalanine hydroxylase, EC 1.14.16.1
q-H_2B	quinonoid 6,7-dihydrobiopterin
SEITU	S-ethyl-isothiourea
SOX	sulfite oxidase
TS	thymidylate synthase
THF	tetrahydrofolate
TrpH	tryptophan hydroxylase, EC 1.14.16.4
TyrH	tyrosine hydroxylase, EC 1.14.16.2
XO	xanthine oxidase

VIII. References

(1) Thony, B.; Auerbach, G.; Blau, N. *Biochem. J.* **2000**, *347*, 1−16.
(2) Werner-Felmayer, G.; Golderer, G.; Werner, E. R. *Curr. Drug Metab.* **2002**, *3*, 159−73.
(3) Fitzpatrick, P. F. *Annu. Rev. Biochem.* **1999**, *68*, 355−381.
(4) Flatmark, T.; Stevens, R. C. *Chem. Rev.* **1999**, *99*, 2137−2160.
(5) Kappock, T. J.; Caradonna, J. P. *Chem. Rev.* **1996**, *96*, 2659−2756.
(6) Gorren, A. C.; Mayer, B. *Curr. Drug Metab.* **2002**, *3*, 133−57.
(7) Wei, C.; Wang, Z.; Meade, A.; McDonald, J.; Stuehr, D. *J. Inorg. Biochem.* **2002**, *91*, 618.
(8) Lovenberg, W.; Levine, R. A. *Unconjugated pterin in neurobiology*; Taylor & Francis, Ltd: Philadelphia, PA, 1987.
(9) Eberlein, G.; Bruice, T. C.; Lazarus, R. A.; Henrie, R.; Benkovic, S. J. *J. Am. Chem. Soc.* **1984**, *106*, 7916−7924.
(10) Thomas, A. H.; Lorente, C.; Capparelli, A. L.; Pokhrel, M. R.; Braun, A. M.; Oliveros, E. *Photochem. Photobiol. Sci.* **2002**, *1*, 421−426.
(11) Kaim, W.; Schwederski, B.; Heilmann, O.; Fridmann, M. H. *Coord. Chem. Rev.* **1999**, *182*, 323−342.
(12) Davis, M. D.; Kaufman, S.; Milstien, S. *Eur. J. Biochem.* **1988**, *173*, 345−351.
(13) Vasquez-Vivar, J.; Whitsett, J.; Martasek, P.; Hogg, N.; Kalyanaraman, B. *Free Radical Biol. Med.* **2001**, *31*, 975−85.
(14) Milstien, S.; Katusic, Z. *Biochem. Biophys. Res. Commun.* **1999**, *263*, 681−4.
(15) Komori, Y.; Hyun, J.; Chiang, K.; Fukuto, J. M. *J. Biochem. (Tokyo)* **1995**, *117*, 923−7.
(16) Toth, M.; Kukor, Z.; Valent, S. *Mol. Hum. Reprod.* **2002**, *8*, 271−80.
(17) Curtius, H. C.; Heintel, D.; Ghisla, S.; Kuster, T.; Leimbacher, W.; Niederwieser, A. *Eur. J. Biochem.* **1985**, *148*, 413−9.
(18) Blair, J. A.; Pearson, A. J. *J. Chem. Soc., Perkin Trans.* **1974**, *2*, 1786−1787.
(19) Armarego, W. L.; Randles, D.; Taguchi, H. *Eur. J. Biochem.* **1983**, *135*, 393−403.
(20) Moad, G.; Luthy, C. L.; Benkovic, P. A.; Benkovic, S. J. *J. Am. Chem. Soc.* **1979**, *101*, 6068−6076.
(21) Lazarus, R. A.; Wallick, D. E.; Dietrich, R. F.; Gottschall, D. W.; Benkovic, S. J.; Gaffney, B. J.; Shiman, R. *Fed. Proc.* **1982**, *41*, 2605−7.
(22) Archer, M. C.; Vonderschmitt, D. J.; Scrimgeour, K. G. *Can. J. Biochem.* **1972**, *50*, 1174−1182.
(23) Gorren, A. C.; Kungl, A. J.; Schmidt, K.; Werner, E. R.; Mayer, B. *Nitric Oxide* **2001**, *5*, 176−86.
(24) Bieri, J. H.; Viscontini, M. *Helv. Chim. Acta* **1977**, *60*, 447−453.
(25) Bieri, J. H.; Viscontini, M. *Helv. Chim. Acta* **1977**, *60*, 1926−1931.
(26) Bieri, J. H. *Helv. Chim. Acta* **1977**, *60*, 2303−2308.
(27) Fontecilla-Camps, J. C.; Bugg, C. E.; Temple, C. J.; Rose, J. D.; Montgomery, J. A.; Kisliuk, R. L. *J. Am. Chem. Soc.* **1979**, *101*, 6114−6115.
(28) Armarego, W. L.; Waring, P. *J. Chem. Res. (S)* **1980**, 318−319.
(29) Weber, R.; Viscontini, M. *Helv. Chim. Acta* **1975**, 1772−1780.
(30) Storm, C. B.; Chung, H. S. *Org. Magn. Reson.* **1976**, *8*, 361−362.
(31) Werner, E. R.; Pitters, E.; Schmidt, K.; Wachter, H.; Werner-Felmayer, G.; Mayer, B. *Biochem. J.* **1996**, *320*, 193−6.
(32) Ziegler, I.; Borchert, M.; Heaney, F.; Davis, A. P.; Boyle, P. H. *Biochim. Biophys. Acta* **1992**, *1135*, 330−4.
(33) Estelberger, W.; Mlekusch, W.; Reibnegger, G. *FEBS Lett.* **1995**, *357*, 37−40.
(34) Estelberger, W.; Fuchs, D.; Murr, C.; Wachter, H.; Reibnegger, G. *Biochim. Biophys. Acta* **1995**, *1249*, 23−8.
(35) Teigen, K.; Dao, K. K.; Froystein, N. A.; Gorren, A. C. F.; Mayer, B.; McKinney, J.; Haavik, J.; Martinez, A. *Chemistry and Biology of Pteridines and Folates*; Kluwer Academic: Boston, MA, 2001.
(36) Martinez, A.; Dao, K. K.; McKinney, J.; Teigen, K.; Froystein, N. A. *Pteridines* **2000**, *11*, 32−33.
(37) Bobst, A. *Helv. Chim. Acta* **1967**, *50*, 2222−2225.
(38) Ehrenberg, A.; Hemmerich, P.; Muller, F.; Pfleiderer, W. *Eur. J. Biochem.* **1970**, *16*, 584−91.
(39) Viscontini, M.; Leidner, H.; Mattern, G.; Okada, T. *Helv. Chim. Acta* **1966**, *49*, 1911−1915.
(40) Funahashi, Y.; Kohzuma, T.; Odani, A.; Yamauchi, O. *Chem. Lett.* **1994**, 385−388.
(41) Eberlein, G.; Bruice, T. C. *J. Am. Chem. Soc.* **1983**, *105*, 6679−6684.
(42) Patel, K. B.; Stratford, M. R.; Wardman, P.; Everett, S. A. *Free Radical Biol. Med.* **2002**, *32*, 203−11.
(43) Kritsky, M. S.; Telegina, T. A.; Lyudnikova, T. A.; Umrikhina, A. V.; Zemskova, Y. *Dokl. Biochem. Biophys.* **2001**, *380*, 336−8.
(44) Kaufman, S.; Pollock, R. J.; Summer, G. K.; Das, A. K.; Hajra, A. K. *Biochim. Biophys. Acta* **1990**, *1040*, 19−27.
(45) Kunz, D. A.; Fernandez, R. F.; Parab, P. *Biochem. Biophys. Res. Commun.* **2001**, *287*, 514−8.
(46) Carreras, C. W.; Santi, D. V. *Annu. Rev. Biochem.* **1995**, *64*, 721−62.
(47) Luykx, D. M.; Duine, J. A.; de Vries, S. *Biochemistry* **1998**, *37*, 11366−75.
(48) Ogura, T.; Yokoyama, T.; Fujisawa, H.; Kurashima, Y.; Esumi, H. *Biochem. Biophys. Res. Commun.* **1993**, *193*, 1014−22.
(49) Silvagno, F.; Xia, H.; Bredt, D. S. *J. Biol. Chem.* **1996**, *271*, 11204−8.
(50) Brenman, J. E.; Xia, H.; Chao, D. S.; Black, S. M.; Bredt, D. S. *Dev. Neurosci.* **1997**, *19*, 224−31.
(51) Elfering, S. L.; Sarkela, T. M.; Giulivi, C. *J. Biol. Chem.* **2002**, *277*, 38079−86.
(52) Abu-Soud, H. M.; Stuehr, D. J. *Proc. Natl. Acad. Sci. U.S.A.* **1993**, *90*, 10769−72.
(53) Roman, L. J.; Martasek, P.; Miller, R. T.; Harris, D. E.; de La Garza, M. A.; Shea, T. M.; Kim, J. J.; Masters, B. S. *J. Biol. Chem.* **2000**, *275*, 29225−32.
(54) Roman, L. J.; Martasek, P.; Masters, B. S. *Chem. Rev.* **2002**, *102*, 1179−1190.
(55) Sono, M.; Roach, M. P.; Coulter, E. D.; Dawson, J. H. *Chem. Rev.* **1996**, *96*, 2841−2888.
(56) Abu-Soud, H. M.; Gachhui, R.; Raushel, F. M.; Stuehr, D. J. *J. Biol. Chem.* **1997**, *272*, 17349−53.
(57) Couture, M.; Stuehr, D. J.; Rousseau, D. L. *J. Biol. Chem.* **2000**, *275*, 3201−5.
(58) Sato, H.; Sagami, I.; Daff, S.; Shimizu, T. *Biochem. Biophys. Res. Commun.* **1998**, *253*, 845−9.
(59) Bec, N.; Gorren, A. C.; Voelker, C.; Mayer, B.; Lange, R. *J. Biol. Chem.* **1998**, *273*, 13502−8.
(60) Rusche, K. M.; Spiering, M. M.; Marletta, M. A. *Biochemistry* **1998**, *37*, 15503−12.
(61) Groves, J. T.; Wang, C. C. *Curr. Opin. Chem. Biol.* **2000**, *4*, 687−95.
(62) Fukuto, J. M. *Methods Enzymol.* **1996**, *268*, 365−75.
(63) Huang, H.; Hah, J. M.; Silverman, R. B. *J. Am. Chem. Soc.* **2001**, *123*, 2674−6.
(64) Adak, S.; Wang, Q.; Stuehr, D. J. *J. Biol. Chem.* **2000**, *275*, 33554−61.
(65) Presta, A.; Siddhanta, U.; Wu, C.; Sennequier, N.; Huang, L.; Abu-Soud, H. M.; Erzurum, S.; Stuehr, D. J. *Biochemistry* **1998**, *37*, 298−310.
(66) Davydov, R.; Ledbetter-Rogers, A.; Martasek, P.; Larukhin, M.; Sono, M.; Dawson, J. H.; Masters, B. S.; Hoffman, B. M. *Biochemistry* **2002**, *41*, 10375−81.
(67) Hurshman, A. R.; Krebs, C.; Edmondson, D. E.; Huynh, B. H.; Marletta, M. A. *Biochemistry* **1999**, *38*, 15689−96.
(68) Hurshman, A. R.; Marletta, M. A. *Biochemistry* **1995**, *34*, 5627−34.
(69) Abu-Soud, H. M.; Wang, J.; Rousseau, D. L.; Fukuto, J. M.; Ignarro, L. J.; Stuehr, D. J. *J. Biol. Chem.* **1995**, *270*, 22997−3006.
(70) Santolini, J.; Adak, S.; Curran, C. M. L.; Stuehr, D. J. *J. Biol. Chem.* **2001**, *276*, 1233−43.
(71) Santolini, J.; Meade, A. L.; Stuehr, D. J. *J. Biol. Chem.* **2001**, *276*, 48887−98.
(72) Tayeh, M. A.; Marletta, M. A. *J. Biol. Chem.* **1989**, *264*, 19654−8.
(73) Kwon, N. S.; Nathan, C. F.; Stuehr, D. J. *J. Biol. Chem.* **1989**, *264*, 20496−501.
(74) Gorren, A. C.; List, B. M.; Schrammel, A.; Pitters, E.; Hemmens, B.; Werner, E. R.; Schmidt, K.; Mayer, B. *Biochemistry* **1996**, *35*, 16735−45.
(75) Klatt, P.; Schmid, M.; Leopold, E.; Schmidt, K.; Werner, E. R.; Mayer, B. *J. Biol. Chem.* **1994**, *269*, 13861−6.
(76) Mayer, B.; Wu, C.; Gorren, A. C.; Pfeiffer, S.; Schmidt, K.; Clark, P.; Stuehr, D. J.; Werner, E. R. *Biochemistry* **1997**, *36*, 8422−7.
(77) Pfeiffer, S.; Gorren, A. C.; Pitters, E.; Schmidt, K.; Werner, E. R.; Mayer, B. *Biochem. J.* **1997**, *328*, 349−52.
(78) List, B. M.; Klosch, B.; Volker, C.; Gorren, A. C.; Sessa, W. C.; Werner, E. R.; Kukovetz, W. R.; Schmidt, K.; Mayer, B. *Biochem. J.* **1997**, *323*, 159−65.
(79) Ghosh, D. K.; Wu, C.; Pitters, E.; Moloney, M.; Werner, E. R.; Mayer, B.; Stuehr, D. J. *Biochemistry* **1997**, *36*, 10609−19.

(80) Werner, E. R.; Habisch, H. J.; Gorren, A. C.; Schmidt, K.; Canevari, L.; Werner-Felmayer, G.; Mayer, B. *Biochem. J.* **2000**, *348*, 579−83.
(81) Kotsonis, P.; Frohlich, L. G.; Raman, C. S.; Li, H.; Berg, M.; Gerwig, R.; Groehn, V.; Kang, Y.; Al-Masoudi, N.; Taghavi-Moghadam, S.; Mohr, D.; Munch, U.; Schnabel, J.; Martasek, P.; Masters, B. S.; Strobel, H.; Poulos, T.; Matter, H.; Pfleiderer, W.; Schmidt, H. H. *J. Biol. Chem.* **2001**, *276*, 49133−41.
(82) Matter, H.; Kotsonis, P.; Klingler, O.; Strobel, H.; Frohlich, L. G.; Frey, A.; Pfleiderer, W.; Schmidt, H. H. *J. Med. Chem.* **2002**, *45*, 2923−41.
(83) Abu-Soud, H. M.; Loftus, M.; Stuehr, D. J. *Biochemistry* **1995**, *34*, 11167−75.
(84) Abu-Soud, H. M.; Wu, C.; Ghosh, D. K.; Stuehr, D. J. *Biochemistry* **1998**, *37*, 3777−86.
(85) Gorren, A. C.; Schmidt, K.; Mayer, B. *Biochemistry* **2002**, *41*, 7819−29.
(86) Gerber, N. C.; Rodriguez-Crespo, I.; Nishida, C. R.; Ortiz de Montellano, P. R. *J. Biol. Chem.* **1997**, *272*, 6285−90.
(87) Renodon, A.; Boucher, J. L.; Wu, C.; Gachhui, R.; Sari, M. A.; Mansuy, D.; Stuehr, D. *Biochemistry* **1998**, *37*, 6367−74.
(88) Gerber, N. C.; Nishida, C. R.; Ortiz de Montellano, P. R. *Arch. Biochem. Biophys.* **1997**, *343*, 249−53.
(89) Wang, J.; Stuehr, D. J.; Rousseau, D. L. *Biochemistry* **1997**, *36*, 4595−606.
(90) Crane, B. R.; Arvai, A. S.; Gachhui, R.; Wu, C.; Ghosh, D. K.; Getzoff, E. D.; Stuehr, D. J.; Tainer, J. A. *Science* **1997**, *278*, 425−31.
(91) Crane, B. R.; Arvai, A. S.; Ghosh, D. K.; Wu, C.; Getzoff, E. D.; Stuehr, D. J.; Tainer, J. A. *Science* **1998**, *279*, 2121−6.
(92) Li, H.; Raman, C. S.; Glaser, C. B.; Blasko, E.; Young, T. A.; Parkinson, J. F.; Whitlow, M.; Poulos, T. L. *J. Biol. Chem.* **1999**, *274*, 21276−84.
(93) Fischmann, T. O.; Hruza, A.; Niu, X. D.; Fossetta, J. D.; Lunn, C. A.; Dolphin, E.; Prongay, A. J.; Reichert, P.; Lundell, D. J.; Narula, S. K.; Weber, P. C. *Nat. Struct. Biol.* **1999**, *6*, 233−42.
(94) Raman, C. S.; Li, H.; Martasek, P.; Kral, V.; Masters, B. S.; Poulos, T. L. *Cell* **1998**, *95*, 939−50.
(95) Pant, K.; Bilwes, A. M.; Adak, S.; Stuehr, D. J.; Crane, B. R. *Biochemistry* **2002**, *41*, 11071−9.
(96) Bird, L. E.; Ren, J.; Zhang, J.; Foxwell, N.; Hawkins, A. R.; Charles, I. G.; Stammers, D. K. *Structure* **2002**, *10*, 1687−96.
(97) Crane, B. R.; Rosenfeld, R. J.; Arvai, A. S.; Ghosh, D. K.; Ghosh, S.; Tainer, J. A.; Stuehr, D. J.; Getzoff, E. D. *EMBO J.* **1999**, *18*, 6271−81.
(98) Siddhanta, U.; Wu, C.; Abu-Soud, H. M.; Zhang, J.; Ghosh, D. K.; Stuehr, D. J. *J. Biol. Chem.* **1996**, *271*, 7309−12.
(99) Panda, K.; Ghosh, S.; Stuehr, D. J. *J. Biol. Chem.* **2001**, *276*, 23349−56.
(100) Sagami, I.; Daff, S.; Shimizu, T. *J. Biol. Chem.* **2001**, *276*, 30036−42.
(101) Crane, B. R.; Arvai, A. S.; Ghosh, S.; Getzoff, E. D.; Stuehr, D. J.; Tainer, J. A. *Biochemistry* **2000**, *39*, 4608−21.
(102) Vasquez-Vivar, J.; Hogg, N.; Martasek, P.; Karoui, H.; Pritchard, K. A., Jr.; Kalyanaraman, B. *J. Biol. Chem.* **1999**, *274*, 26736−42.
(103) Boggs, S.; Huang, L.; Stuehr, D. J. *Biochemistry* **2000**, *39*, 2332−9.
(104) Wei, C. C.; Wang, Z. Q.; Wang, Q.; Meade, A. L.; Hemann, C.; Hille, R.; Stuehr, D. J. *J. Biol. Chem.* **2001**, *276*, 315−9.
(105) Szalai, V. A.; Kuhne, H.; Lakshmi, K. V.; Brudvig, G. W. *Biochemistry* **1998**, *37*, 13594−603.
(106) Schmidt, P. P.; Lange, R.; Gorren, A. C.; Werner, E. R.; Mayer, B.; Andersson, K. K. *J. Biol. Inorg. Chem.* **2001**, *6*, 151−8.
(107) Du, M.; Yeh, H. C.; Berka, V.; Wang, L. H.; Tsai, A. L. *J. Biol. Chem.* **2003**, *278*, 6002−11.
(108) Rees, D. C.; Hu, Y.; Kisker, C.; Schindelin, H. *J. Chem. Soc., Dalton Trans.* **1997**, 3909−3914.
(109) Wei, C. C.; Wang, Z. Q.; Arvai, A. S.; Hemann, C.; Hille, R.; Getzoff, E. D.; Stuehr, D. J. *Biochemistry* **2003**, *42*, 1969−1977.
(110) Armstrong, D. A.; Farahani, M.; Surdhar, P. S. *Can. J. Chem.* **1990**, *68*, 1974.
(111) Fritz, T. A.; Liu, L.; Finer-Moore, J. S.; Stroud, R. M. *Biochemistry* **2002**, *41*, 7021−9.
(112) Barrett, J. E.; Lucero, C. M.; Schultz, P. G. *J. Am. Chem. Soc.* **1999**, *121*, 7965−7966.
(113) Nocek, J. M.; Zhou, J. S.; DeForest, S.; Pryadarsky, S.; Beratan, D. N.; Onuchic, J. N.; Hoffman, B. M. *Chem. Rev.* **1996**, *96*, 2459−2489.
(114) Musah, R. A.; Jensen, G. M.; Bunte, S. W.; Rosenfeld, R. J.; Goodin, D. B. *J. Mol. Biol.* **2002**, *315*, 845−857.
(115) Gorren, A. C.; Schrammel, A.; Riethmuller, C.; Schmidt, K.; Koesling, D.; Werner, E. R.; Mayer, B. *Biochem. J.* **2000**, *347*, 475−84.
(116) Riethmuller, C.; Gorren, A. C.; Pitters, E.; Hemmens, B.; Habisch, H. J.; Heales, S. J.; Schmidt, K.; Werner, E. R.; Mayer, B. *J. Biol. Chem.* **1999**, *274*, 16047−51.
(117) Hevel, J. M.; Marletta, M. A. *Biochemistry* **1992**, *31*, 7160−5.
(118) Gorren, A. C.; Bec, N.; Schrammel, A.; Werner, E. R.; Lange, R.; Mayer, B. *Biochemistry* **2000**, *39*, 11763−70.
(119) Presta, A.; Weber-Main, A. M.; Stankoivh, M. T.; Stuehr, D. J. *J. Am. Chem. Soc.* **1998**, *120*, 9560−9565.
(120) Stuehr, D.; Pou, S.; Rosen, G. M. *J. Biol. Chem.* **2001**, *276*, 14533−6.
(121) Rosen, G. M.; Tsai, P.; Weaver, J.; Porasuphatana, S.; Roman, L. J.; Starkov, A. A.; Fiskum, G.; Pou, S. *J. Biol. Chem.* **2002**, *277*, 40275−80.
(122) Bec, N.; Gorren, A. F. C.; Mayer, B.; Schmidt, P. P.; Andersson, K. K.; Lange, R. *J. Inorg. Biochem.* **2000**, *81*, 207−11.
(123) Hurshman, A. R.; Marletta, M. A. *Biochemistry* **2002**, *41*, 3439−56.
(124) Chen, P. F.; Tsai, A. L.; Berka, V.; Wu, K. K. *J. Biol. Chem.* **1997**, *272*, 6114−8.
(125) Ghosh, S.; Wolan, D.; Adak, S.; Crane, B. R.; Kwon, N. S.; Tainer, J. A.; Getzoff, E. D.; Stuehr, D. J. *J. Biol. Chem.* **1999**, *274*, 24100−12.
(126) Sato, Y.; Sagami, I.; Shimizu, T. *J. Inorg. Biochem.* **2001**, *87*, 261−6.
(127) Chen, P. F.; Berka, V.; Wu, K. K. *Arch. Biochem. Biophys.* **2003**, *411*, 83−92.
(128) Wang, Z. Q.; Wei, C. C.; Ghosh, S.; Meade, A. L.; Hemann, C.; Hille, R.; Stuehr, D. J. *Biochemistry* **2001**, *40*, 12819−25.
(129) Eberlein, G.; Bruice, T. C. *J. Am. Chem. Soc.* **1983**, *105*, 6685−6697.
(130) Aoyagi, M.; Arvai, A. S.; Ghosh, S.; Stuehr, D. J.; Tainer, J. A.; Getzoff, E. D. *Biochemistry* **2001**, *40*, 12826−32.
(131) Dougherty, D. A. *Science* **1996**, *271*, 163−8.
(132) Mecozzi, S.; West, A. P., Jr.; Dougherty, D. A. *Proc. Natl. Acad. Sci. U.S.A.* **1996**, *93*, 10566−71.
(133) Shi, Z.; Olson, C. A.; Kallenbach, N. R. *J. Am. Chem. Soc.* **2002**, *124*, 3284−91.
(134) Abu-Soud, H. M.; Ichimori, K.; Presta, A.; Stuehr, D. J. *J. Biol. Chem.* **2000**, *275*, 17349−57.
(135) Iwanaga, T.; Yamazaki, T.; Kominami, S. *Biochemistry* **1999**, *38*, 16629−35.
(136) Wang, Z. Q.; Wei, C. C.; Stuehr, D. J. *J. Biol. Chem.* **2002**, *277*, 12830−7.
(137) Moran, G. R.; Daubner, S. C.; Fitzpatrick, P. F. *J. Biol. Chem.* **1998**, *273*, 12259−66.
(138) Fitzpatrick, P. F. In *Advances in Enzymology and Related Areas of Molecular Biology*; Purich, D. L., Ed.; John Wiley & Sons: New York, 2000.
(139) Dix, T. A.; Benkovic, S. J. *Biochemistry* **1985**, *24*, 5839−46.
(140) Davis, M. D.; Kaufman, S. *J. Biol. Chem.* **1989**, *264*, 8585−96.
(141) Kaufman, S. *Adv. Enzymol. Relat. Areas Mol. Biol.* **1993**, *67*, 77−264.
(142) Andersen, O. A.; Flatmark, T.; Hough, E. *J. Mol. Biol.* **2001**, *314*, 279−91.
(143) Andersen, O. A.; Flatmark, T.; Hough, E. *J. Mol. Biol.* **2002**, *320*, 1095−108.
(144) Goodwill, K. E.; Sabatier, C.; Stevens, R. C. *Biochemistry* **1998**, *37*, 13437−45.
(145) Wang, L.; Erlandsen, H.; Haavik, J.; Knappskog, P. M.; Stevens, R. C. *Biochemistry* **2002**, *41*, 12569−74.
(146) Fusetti, F.; Erlandsen, H.; Flatmark, T.; Stevens, R. C. *J. Biol. Chem.* **1998**, *273*, 16962−7.
(147) Hagedoorn, P. L.; Schmidt, P. P.; Andersson, K. K.; Hagen, W. R.; Flatmark, T.; Martinez, A. *J. Biol. Chem.* **2001**, *276*, 22850−6.
(148) Erlandsen, H.; Stevens, R. C. *Mol. Genet. Metab.* **1999**, *68*, 103−25.
(149) Erlandsen, H.; Bjorgo, E.; Flatmark, T.; Stevens, R. C. *Biochemistry* **2000**, *39*, 2208−17.
(150) Erlandsen, H.; Kim, J. Y.; Patch, M. G.; Han, A.; Volner, A.; Abu-Omar, M. M.; Stevens, R. C. *J. Mol. Biol.* **2002**, *320*, 645−61.
(151) Bassan, A.; Blomberg, M. R.; Siegbahn, P. E. *Chemistry* **2003**, *9*, 106−15.
(152) Schindelin, H.; Kisker, C.; Rajagopalan, K. V. In *Advances in Protein Chemistry*; Richard, F. M., Eisenberg, D. S., Eds.; Academic Press: New York, 2001; Vol. 58.
(153) Kisker, C.; Schindelin, H.; Baas, D.; Retey, J.; Meckenstock, R. U.; Kroneck, P. M. H. *FEMS Microbiol. Rev.* **1999**, *22*, 503−521.
(154) Kisker, C.; Schindelin, H.; Rees, D. C. *Annu. Rev. Biochem.* **1997**, *66*, 233−67.
(155) Rees, D. C. *Annu. Rev. Biochem.* **2002**, *71*, 221−46.
(156) McAlpine, A. S.; McEwan, A. G.; Shaw, A. L.; Bailey, S. *JBIC* **1997**, *2*, 690−701.
(157) Schindelin, H.; Kisker, C.; Hilton, J.; Rajagopalan, K. V.; Rees, D. C. *Science* **1996**, *272*, 1615−21.
(158) Schneider, F.; Lowe, J.; Huber, R.; Schindelin, H.; Kisker, C.; Knablein, J. *J. Mol. Biol.* **1996**, *263*, 53−69.
(159) Dias, J. M.; Than, M. E.; Humm, A. E.; Huber, R.; Bourenkov, G. P.; Bartunik, H. D.; Bursakov, S.; Calvete, J.; Caldeira, J.; Carneiro, C. *Structure* **1999**, *7*, 65−79.
(160) Boyington, J. C.; Gladyshev, V. N.; Khangulov, S. V.; Stadtman, T. D.; Sun, P. D. *Science* **1997**, *275*, 1305−1308.

(161) Jormakka, M.; Tornroth, S.; Byrne, B.; Iwata, S. *Science* **2002**, *295*, 1863−1868.
(162) Enroth, C.; Eger, B. T.; Okamato, K.; Nishino, T.; Pai, E. F. *Proc. Natl. Acad. Sci. U.S.A.* **2000**, *97*, 10723−10728.
(163) Huber, R.; Hof, P.; Duarte, R. O.; Moura, J. J. G.; Moura, I.; Liu, M.-Y.; LeGall, J.; Hille, R.; Archer, M.; Romao, M. J. *Proc. Natl. Acad. Sci. U.S.A.* **1996**, *17*, 8846−8851.
(164) Romao, M. J.; Archer, M.; Moura, I.; LeGall, J.; Engh, R.; Schneider, M.; Hof, P.; Huber, R. *Science* **1995**, *270*, 1170−1176.
(165) Dobbek, H.; Gremer, L.; Meyer, O.; Huber, R. *Proc. Natl. Acad. Sci. U.S.A.* **1999**, *96*, 8884−8889.
(166) Nishino, T.; Okamoto, K. *J. Inorg. Biochem.* **2000**, *82*, 43−9.
(167) Hu, Y.; Faham, S.; Roy, R.; Adams, R. W. W.; Rees, D. C. *J. Mol. Biol.* **1999**, *286*, 899−914.
(168) Chen, P. F.; Berka, V.; Tsai, A. L.; Wu, K. K. *J. Biol. Chem.* **1998**, *273*, 34164−70.

CR0204350